UNIVERSIDADE DE LISBOA
FACULDADE DE CIÊNCIAS
DEPARTAMENTO DE ENGENHARIA GEOGRÁFICA, GEOFÍSICA E ENERGIA

Vegetation recovery in Portugal following large wildfire episodes

Ana Filipa Ferreira Bastos

Mestrado Integrado em Engenharia da Energia e do Ambiente

2011

UNIVERSIDADE DE LISBOA
FACULDADE DE CIÊNCIAS
DEPARTAMENTO DE ENGENHARIA GEOGRÁFICA, GEOFÍSICA E ENERGIA

Vegetation recovery in Portugal following large wildfire episodes

Ana Filipa Ferreira Bastos

Mestrado Integrado em Engenharia da Energia e do Ambiente

Trabalho realizado sob a supervisão de

Célia Gouveia (IDL)

Carlos da Camara (FCUL)

2011

Abstract

As in the Mediterranean ecosystems, fire regimes in Portugal, , have been changing due to land-use modifications and climatic warming. Fire has become an important ecosystems' disturbance, leading to soil impoverishment and desertification. In the European Mediterranean context, Portugal has registered the highest number of fire occurrences since 1980 and the larger burnt area over the past decade. Thus, an exhaustive study of vegetation recovery after fire events becomes crucial in land management. Two outstanding fire seasons were recorded in Portugal in 2003 and 2005, which coincided with extreme climatic events, a strong heat wave in 2003 and, in 2004/2005, one of the most severe droughts since early 20th century.

The aim of the present study is to i) discriminate large burnt scars in Portugal during the 2003, 2004 and 2005 fire seasons, ii) monitor vegetation behaviour throughout the pre and the post fire periods and iii) identify physical and environmental factors driving post-fire recovery. The study makes extensive use of the mono-parametric model developed by Gouveia et al. (2010), based on monthly values of NDVI from 1998 to 2009, at 1km×1km spatial scale, as obtained from the VEGETATION-SPOT5 instrument. The model was previously validated and some corrections introduced. The proposed procedure allows identifying burnt scars, estimating vegetation recovery times for each scar and assessing the influence of fire damage, pre-fire vegetation density, plant traits and terrain characteristics on post-fire vegetation recovery.

Resumo

Em Portugal, tal como em outros ecossistemas Mediterrânicos, tem-se registado um aumento quer no número de fogos, quer na extensão de área ardida. As alterações observadas nos regimes de fogo ao longo das últimas décadas devem-se sobretudo a mudanças no uso do solo, nomeadamente ao abandono rural e à mecanização da agricultura, que conduziram à acumulação de material combustível e à homogeneização da paisagem, bem como às alterações climáticas, que se caracterizam não só por um aumento da temperatura, mas também por um incremento na frequência de fenómenos extremos, tais como secas e ondas de calor. Estas alterações, quando combinadas, provocam um aumento do risco de incêndio. Portugal é um caso paradigmático no contexto da Europa Mediterrânica, registando o número mais elevado de fogos desde 1980, bem como a maior extensão de área ardida na última década. Em 2003 e 2005 Portugal assistiu a duas épocas de incêndios extraordinárias, que coincidiram com fenómenos climáticos extremos: uma forte onda de calor, em 2003, e uma das mais prolongadas secas da década, em 2004/2005. Nestas duas épocas de incêndios registaram-se os dois máximos de área ardida desde 1980, com 425000 ha ardidos em 2003 e 338000 ha em 2005. Em 2005 registou-se igualmente o valor máximo para o número de fogos em Portugal desde 1980.

Apesar de a paisagem mediterrânica ter evoluído ao longo de milhares de anos em conjunto com o fogo, este constitui actualmente umas das suas maiores perturbações ecológicas, sendo responsável pelo empobrecimento dos solos, devido à perda de nutrientes; pela redução da camada de vegetação e consequentemente o aumento da erosão; e por transformações dos processos hidro-ecológicos da região.

A vegetação mediterrânica é caracterizada por uma elevada capacidade de adaptação a fogos, através de estratégias de recuperação depois de incêndios. Certas espécies regeneram a partir de estruturas resistentes ao fogo, como é o caso do sobreiro (*Quercus Suber*), enquanto outras espécies apostam no estímulo da reprodução pós-fogo, através de sementes resistentes a elevadas temperaturas, como é o caso do pinheiro-bravo (*Pinus Pinaster*). No entanto, nem todas as espécies mediterrânicas logram recuperar depois de incêndios, e mesmo as espécies adaptadas ao fogo revelam uma redução na sua capacidade de recuperação após fogos recorrentes. A recuperação da vegetação depois de um fogo é um fenómeno complexo, que depende de diversas variáveis, nomeadamente a severidade do fogo, a densidade da vegetação antes do fogo e o tipo de vegetação, e de outros factores ambientais. A disponibilidade de água é um factor determinante na actividade da vegetação, sendo a recuperação da vegetação afectada pela quantidade de água no solo que, por sua vez, depende de factores climáticos, como a precipitação e temperatura, e das características do terreno, como o declive (vertentes viradas a Norte têm menos perdas por evapo-transpiração) e a altitude. Dada a sua complexidade, o estudo aprofundado da recuperação da vegetação após grandes fogos é determinante para um correcto planeamento de medidas de prevenção da erosão, bem como para o ordenamento do território e gestão das florestas.

A Detecção Remota tem-se revelado um instrumento particularmente útil neste contexto, já que facilita o mapeamento de fogos e permite analisar a dinâmica da vegetação, bem como avaliar situações de stress, em áreas extensas e durante períodos temporais relativamente longos, com custos reduzidos.

Os principais objectivos deste trabalho são i) efectuar uma análise preliminar da sensibilidade do modelo de recuperação da vegetação, desenvolvido por Gouveia et al. (2010), à dimensão da janela temporal, a dados em falta e a perturbações na actividade da vegetação; ii) analisar áreas ardidas nas épocas de incêndio de 2003, 2004 e 2005 e monitorizar a actividade da vegetação antes e depois da ocorrência do fogo através da aplicação do modelo à série temporal do Índice de Vegetação por Diferenças Normalizadas (*Normalized Difference Vegetation Index*, NDVI); e iii) e proceder a uma identificação dos factores físicos e ambientais que determinam a recuperação da vegetação depois de um fogo. O estudo baseia-se em valores mensais do NDVI, obtidos através do sensor VEGETATION-SPOT5, com resolução espacial de 1kmx1km, compreendidos num período entre 1998 e 2009.

A metodologia utilizada permitiu identificar as áreas ardidas referentes às épocas de incêndio estudadas, que foram validadas de acordo com os dados oficiais para as áreas ardidas. A implementação do modelo em certas áreas revelou um problema de ajuste do ponto inicial, já que o mínimo de NDVI era atingido alguns meses depois do incêndio, tal se devendo ao facto de as

condições adversas observadas durante os meses de outono e inverno conduzirem a um acréscimo da mortalidade da vegetação que sobreviveu ao incêndio.

Dado que em Gouveia e tal. (2010) a série temporal disponível não permitia a observação de uma total recuperação da vegetação, a validade do modelo foi inicialmente testada, através da comparação entre os tempos de recuperação estimados em Gouveia e tal. (2010) e os estimados através da série temporal mais alargada, utilizada no presente trabalho (1998-2009). Verificou-se que o modelo implementado fornece, em geral, estimativas de tempos de recuperação muito próximos dos observados. No entanto, para determinadas áreas ardidas, verificaram-se perturbações no ciclo vegetativo durante o processo de recuperação que, naturalmente, o modelo não poderia prever. Assim, incluiu-se uma correcção para que estes valores fossem retirados da análise de regressão, dado que poderiam introduzir variabilidade fenológica. Foi também avaliada a sensibilidade do modelo a dados em falta ao longo da série temporal. Verificou-se que o modelo é pouco sensível à falta de alguns valores de NDVI depois da ocorrência do incêndio se o processo de recuperação for regular, apresentando desvios muito reduzidos nas estimativas de tempo de recuperação. No entanto, a existência de perturbações na dinâmica da vegetação durante o período de recuperação, ou mesmo vários anos depois, conduz a erros de magnitude considerável nas estimativas do modelo. A seca constitui uma destas perturbações no processo de recuperação, pelo que o seu efeito sobre as estimativas do modelo foi avaliado. Verificou-se que, nas áreas afectadas em grande magnitude pela seca de 2004/05, a análise de regressão foi enviesada pela presença de vários meses com actividade vegetativa reduzida.

Foram seleccionadas quatro áreas, correspondentes às três épocas de incêndios consideradas e localizadas em diversas regiões de Portugal Continental, para que se pudesse estudar o processo de recuperação de forma mais aprofundada, nomeadamente a influência de diversos factores físicos, ecológicos e geomorfológicos e identificar aqueles que determinam o processo de recuperação. Foi avaliada a influência da severidade do fogo, da densidade de vegetação antes do fogo, do tipo de vegetação e ainda da orientação do declive do terreno, sendo possível verificar a existência de comportamentos distintos. Observou-se que a regeneração das áreas compostas por florestas de pinheiro-bravo era tendencialmente lenta, tendo-se revelado marcadamente influenciada pela severidade do fogo, bem como pela disponibilidade de água no solo, influenciada, por sua vez, pela orientação do declive do terreno. As folhosas (sobreiros) apresentaram tempos de recuperação muito curtos (inferiores a dois anos) e o seu processo de recuperação mostrou-se ligeiramente influenciado pela densidade de vegetação pré-fogo, sendo independente de qualquer um dos outros factores analisados. Verificou-se ainda que, em geral, a vegetação arbustiva ou de transição recuperava rapidamente depois do fogo. Estes resultados são consistentes com as características adaptativas de recuperação após um fogo correspondentes a cada um dos tipos de vegetação estudados. Desta forma, observa-se que a metodologia implementada, não só é válida para obter estimativas dos tempos de recuperação de áreas ardidas, como também permite uma análise mais aprofundada da recuperação da vegetação, nomeadamente o estudo da influência de factores físicos, ambientais e climáticos no processo de regeneração pós-fogo da vegetação. No entanto, esta análise não dispensa a realização de estudos complementares, de campo ou recorrendo a outros índices, sempre que seja necessário avaliar a evolução da composição ou estrutura do ecossistema depois de um incêndio.

Keywords: NDVI, Vegetation recovery, Fire, Mediterranean.

Palavras-chave: NDVI, Recuperação da vegetação, Fogo, Mediterrâneo.

Index

Abstract 5

Resumo 7

Keywords: 8

1. Introduction 1

2. Data and Pre-Processing 5

2.1 Normalized Difference Vegetation Index 5

2.2 NDVI Data and pre-processement 6

2.3 Land-cover data 8

2.4 Digital elevation model 9

3. Vegetation recovery 10

3.1 Burnt areas identification 10

3.2 Model of post-fire vegetation recovery 13

3.2.1 Adjustment to the starting point 16

3.2.2 Application of the model to an extended dataset 17

3.2.3 Sensitivity to missing data 20

3.2.4 Sensitivity to drought 24

4. Case-studies 27

4.1 Region III 27

4.2 Region V 31

4.3 Region VII 34

4.4 Region IX 37

4.5 Slope dependence 41

5. Conclusions and final remarks 43

6. References 46

List of Figures

Fig. 1 – Normalized reflectance spectra for several non-vegetated areas (panel a) and for different types of vegetated land-cover (panel b) (Myneni et al., 1995). 5
Fig. 2 – MVC-NDVI (black dots) and the fitted EFAI-NDVI time series (red line) for the hydrological year of 2001, averaged over Continental Portugal for all pixels (left panel), broad-leaved and mixed forest pixels (central panel) and pixels of arable land (right panel). 7
Fig. 3 – EFAI-NDVI time-series averaged over Continental Portugal for all pixels (black line), for pixels of broad-leaved and mixed forest (green line) and for pixels of arable land (red line). Time-series starts on the second decade of August 1998 and ends on the first decade of August 2009. Vertical dotted lines indicate the month of January for each year. Black arrows point the drought episodes of 1999, 2002 and 2005. 7
Fig. 4 – Corine Land-cover 2000 map for Continental Portugal as developed by ISEG at 250m spatial resolution (left) and land-cover classes and nomenclature (right). 8
Fig. 5 – Digital Elevation Model for Continental Portugal at 1km spatial resolution, corrected to fit MVC-NDVI data coordinates. Vertical units represent elevation in meters above mean sea level. 9
Fig. 6 – Burnt areas (black pixels) in Continental Portugal during the 2003 fire season (left panel), as identified by a cluster analysis of MVC-NDVI anomalies throughout the 2004 hydrological year (right panel). Time series of two identified centroids of identified, associated to burnt pixels (bold line with open circles) and to non-burnt pixels (black asterisks). 10
Fig. 7 – Burnt areas (black pixels) in Continental Portugal during the 2004 fire season as identified by cluster analysis (left panel) and corrected by removing pixels from the fires of 2003 fire season (centre panel. Cluster analysis was performed on MVC-NDVI anomalies throughout the 2005 hydrological year (right panel). Four clusters were identified, being the one with centroid with large negative values in the first months associated to burnt pixels (bold line with open circles), and the others to non-burnt pixels (black asterisks). 11
Fig. 8 – As in Fig. 7 but respecting to the 2005 fire season. Four clusters were identified, being the one with centroid with large negative values in the first months associated to burnt pixels (bold line with open circles), and the others to non-burnt pixels (black asterisks). 11
Fig. 9 – Burnt areas in Continental Portugal for the 2000-2004 period as identified by AFN, based on Landsat imagery (left panel). Burnt areas in Continental Portugal for the 2003 (orange pixels), 2004 (green pixels) and 2005 (red pixels) fire seasons as obtained by the cluster analysis of the NDVI anomalies over the year following each fire season (central panel). Burnt areas in Continental Portugal for 2005 as identified by AFN, based on Modis imagery (right panel). 12
Fig. 10 - Burnt areas in Continental Portugal for the 2003 (orange pixels), 2004 (green pixels) and 2005 (red pixels) fire seasons as obtained by the cluster analysis of the NDVI anomalies over the year following each fire season (left panel). Corine Land-cover 2000 map for Continental Portugal

developed by ISEG at 250m spatial resolution (right panel). Selected areas for the present work are identified by labels associated to rectangular frames. 13
Fig. 11 – Time series of NDVI (grey curves) spatially averaged over the two selected large fire scars respectively located in Region I (upper panel) and in Region II (lower panel). Black curves represent the Gorgeous Years (GY) of vegetation, given by the annual cycles of maximum NDVI for each month over the considered period. Vertical dotted lines indicate the month of January for each year. (Gouveia et al. 2010) 15
Fig. 12– Time series of observed (lines with asterisks) and modelled (bold curves) values of monthly values of lack of greenness, *y*, over the large fire scars located in Region 1 (upper panel) and in Region II (lower panel). The dashed curves indicate the 95% confidence limits of the regressed curve and the large grey circles indicate the annual means of *y*. The horizontal dotted line represents the level of vegetation recovery defined as 90% of the mean value of *y* during the pre fire period (represented, in turn, by the horizontal solid line). Arrows indicate the estimated recovery dates, defined as the instant when the modelled curves of *y* cross the level of vegetation recovery. Vertical dotted lines indicate the month of January for each year. (Gouveia et al. 2010) 15
Fig. 13 – Time-series of observed (black line with asterisks) and modelled (black line) *y* time-series averaged over the burnt scar in Region VI without correction (top right panel) and corrected (bottom right panel). Red ellipse (upper right panel) highlights the misadjustment of the uncorrected modelled curve vegetation recovery. Vertical arrows indicate vegetation recovery..... 16
Fig. 14– Time series of NDVI (grey curve) and of GY (black curve) spatially averaged over Region II (left panel), and Region IV (right panel). 17
Fig. 15 – Lack of greenness, *y*, time-series (black line with asterisks) and modelled curve (solid line) of vegetation recovery, spatially averaged over Region II (left panel) and Region IV (right panel). ... 17
Fig. 16 – As in Fig. 15 but respecting to Region II (top panel) and Region IV (bottom panel) for distinct periods corresponding to criteria (i) (black), (ii) (blue) and (iii) (green). Red lines indicate 95% confidence limits of the regressed curve (i). For GII, *y* time-series and modeled curves (ii) and (iii) are coincident. 18
Fig. 17 – As in Fig. 16 but respecting to the burnt scar in Region I. 20
Fig. 18 – As in Fig. 15 but respecting to the burnt scar in Region VIII. 21
Fig. 19 – As in Fig. 15 but respecting to the burnt scar in Region VIII, tested for the four hypotheses of missing data: a) missing values distributed randomly over the period after the fire event (upper left panel); b) data missing for the year following the month of fire (upper right panel); c) data missing during the recovery period, in the second year following the fire (lower left panel); d) data missing after complete recovery, in the third year after the fire(lower right panel). 21
Fig. 20 – As in Fig. 15 but respecting to the burnt scar in Region I, when tested with the three cases of missing data in Table 3. 23
Fig. 21 – As in Fig. 15 but respecting to the burnt scars in Region III (top panel) and Region IV (bottom panel). Red ellipses indicate the effect of the 2005 drought. 24

Fig. 22 – Monthly NDVI anomaly time-series (upper panel) averaged over the burnt area in Region III, (black line), and over the corresponding control area (blue line). The dashed red line indicates NDVI anomaly threshold of -0.025. Red vertical lines and horizontal arrow indicate the drought period. Time-series of observed (black line with asterisks) and modelled (black line) NDVI anomaly and time-series of the lack of greenness (lower panel), spatially averaged over the burnt scar, after setting values corresponding to the drought period as no-value data. 25
Fig. 23 – As in Fig. 22, but respecting the burnt area IV. 26
Fig. 24 – Land-cover map over the burnt scar (413 pixels) in Region III, according to CLC 2000 classes shown in the colorbar. 27
Fig. 25- NDVI (grey line) and GY (black line) time-series (left panel) spatially averaged over the burnt scar in Region III. Time-series of observed (black line with asterisks) and modelled (black curve) lack of greenness, averaged over the burnt area (right panel). Red curves indicate 95% confidence limits of the regressed curve and red circles indicate annual means of *y*. 28
Fig. 26 – Mean NDVI fields over burnt scar in Region III on May of 2003, 2004 and 2008. 28
Fig. 27–Spatial distribution of recovery times (in months) as estimated by applying the described methodology to each pixel. 29
Fig. 28 – Dispersion diagrams (upper panels) and spatial distribution (lower panels) of clusters, identified by distinct colors, as obtained by applying the K-means clustering to the pairs $\{t_R, NDVI_{2004}\}$ (left panels) and $\{t_R, NDVI_{MEDIAN}\}$ (right panels), for Region III. Coordinates of the centroids of each cluster are identified by circles in the dispersion diagrams; horizontal and vertical bars indicate interquartile ranges. Integer numbers near each centroid indicate the fraction of areal cover (%) by each cluster. 29
Fig. 29 – Land-cover map over the burnt scar (382 pixels) in Region V, according to CLC 2000 classes shown in the colorbar. 31
Fig. 30 – As in Fig. 21 but respecting to the fire scar in Region V. 31
Fig. 31 – As in Fig. 22 but respecting to the fire scar in Region V. 32
Fig. 32 – As in Fig. 23 but respecting to the fire scar in Region V. 32
Fig. 33 – As in Fig. 24 but respecting to the fire scar in Region V. 33
Fig. 34 – Land-cover map over the burnt scar (257 pixels) in Region VII, according to CLC 2000 classes shown in the colorbar. 34
Fig. 35 – As in Fig. 21 but respecting to the fire scar in Region VII. 35
Fig. 36– As in Fig. 22, but respecting to the fire scar in Region VII. 35
Fig. 37 – As in Fig. 23, but respecting to the fire scar in Region VII. 35
Fig. 38 – As in Fig. 24, but respecting to the fire scar in Region VII 36
Fig. 39 – Land-cover map over the burnt scar (105 pixels) in Region IX, according to CLC 2000 classes shown in the colorbar. 37
Fig. 40 – As in Fig. 21 but respecting to the fire scar in Region IX. 38
Fig. 41 – As in Fig. 22 but respecting to the fire scar in Region IX. 38

Fig. 42 – As in Fig. 23 but respecting to the fire scar in Region IX. 38
Fig. 43 – As in Fig. 24 but respecting to the fire scar in Region IX. 39
Fig. 44 – Recovery time distribution over each slope aspect (North and South) for Regions III, V, VII and IX. Red lines indicate median values; blue boxes indicate the 25% and 75% interquartile ranges and black whiskers encompass the 1.5% and 98.5% interquartile ranges. Red crosses represent outliers. 42

List of Tables

Table 1 – Estimates (t_R) and 95% confidence intervals ($I_{95}[t_R]$) of recovery time respecting to the fit by linear regression of the mono-parametric model of vegetation recover using criteria (i), (ii) and (iii, in all selected Regions. 19
Table 2 - Vegetation recovery time (t_R) and respective 95% confidence interval ($I_{95}[t_R]$), in months, as estimated by the mono-parametric vegetation recovery model for the burnt scar in Region VIII, for the baseline (no missing data) and for the four cases of missing data as shown in Fig.15, where t_0 is defined as the month use to set parameter *a* of the regression. 22
Table 3 – As in Table 2 but respecting to the burnt scar in Region I for the baseline (no missing data) and for the cases of missing data after the first year of recovery and of missing data in the last twelve months of the time series. 22
Table 4 – Vegetation recovery time (t_R) and respective 95% confidence interval ($I_{95}[t_R]$), as estimated by the mono-parametric vegetation recovery model for the burnt scars in Regions III and IV. Vegetation recovery time (t_R*) and 95% confidence interval ($I_{95}[t_R]$*),as estimated by the mono-parametric vegetation recovery model after setting the values of observed lack of greenness corresponding to the drought period as missing data. 26
Table 5 – Land-cover distribution over the three centroids as identified by the cluster analysis of the recovery time for Region III. 30
Table 6 – As in Table 5 but respecting fire scar in Region V. 33
Table 7 – As in Table 5, but respecting to Region VII. 37
Table 8 – As in Table 5, but respecting to Region IX. 40
Table 9 – Statistical distribution (median, lower and upper quartiles) of the computed slope, given in percentage (%), over each burnt scar, for the North and South facing hillsides. 41

1. Introduction

Fire is a natural factor affecting many ecosystems, including the Mediterranean ones which are well adapted to recover after wildfires. However, fire regimes in the European Mediterranean areas have been changing in the last decades, mainly due to land-use changes and climatic warming. Fire events in this region have markedly increased in the last decades, both in number and surface burnt, becoming a serious problem and a major ecosystem disturbance, increasing erosion and soil degradation.

Vegetation patterns in the Mediterranean basin have evolved in deep connection with human activity and land-use throughout many centuries (Naveh, 1975). In this particular, European industrialization induced several changes in rural areas, such as depopulation, decreases in grazing pressure and wood gathering, agriculture mechanization, and land abandonment that led to landscape homogenization and fuel accumulation. These changes seem to be the main reason for the increasing number and extension of wildfires in recent decades (Röder et al., 2008), since the same trends are not observed in southern Mediterranean areas, where traditional land-uses are still relevant (Pausas and Vallejo, 1999). On the other hand the Mediterranean basin is particularly sensitive to climate change, and an increase in average temperature together with a reduction of summer rainfall is expected (Houghton et al. 1996), which may increase water stress and fire risk. Terrestrial ecosystems play in turn a crucial role in global climate dynamics, since they are an important part of geobiochemical cycles, such as CO_2, methane or nitrous oxide, that are powerful greenhouse gases. Biomass is a major reservoir of carbon, which is rapidly released to the atmosphere in the form of CO_2 whenever vegetation or organic matter is burnt. Large wildfires turn forests from sinks into great sources of greenhouse gases emissions, with feedback effects that are extremely complex and difficult to model.

Fires play an important role in biological productivity and composition of Mediterranean ecosystems, but may also be responsible for soil degradation and desertification. Main fire impacts on ecosystems consist on (i) soil impoverishment through loss of nutrients during the fire event or after, by runoff; (ii) loss of plant cover and, consequently, erosion; and (iii) changes in hydro-ecological processes (Moreno and Oechel, 1995; Inbar et al., 1998). Whether vegetation recovery decreases post-fire runoff and erosion in the long-term, in the short term autumn rainstorms increase erosion and nutrient loss after summer fires (De Luís et al., 2001). Thornes (1990) suggested that a minimum of 30% of vegetation cover is required to protect the soil against water erosion. The majority of sediment loss seems to occur in the first year after fire (DeBano et al., 1998; Cerdà and Doerr, 2005) and the risk of post-fire soil erosion increases with the time required for vegetation to reach the minimal threshold (Shakesby et al., 1993; Cerdà, 1998; Inbar et al., 1998).

Fires have complex effects on vegetation recovery, which depend on fire regimes and characteristics, e.g. intensity, seasonality, recurrence and extent (Naveh, 1995), on the vegetation response to such regimes and on environmental factors, like terrain and climate (De Luís et al., 2001, 2004).

Some of the Mediterranean vegetation species have developed adaptation strategies to wild fires, which aim at individual survival and post-fire reproduction stimulation. Individual survival can be accomplished by isolation tissues or by resprouting. The majority of pine and oak species rely on a thick bark to ensure protection against the high temperatures reached during a fire event. *Pinus pinaster*, for instance, has a laminated bark which is exfoliated during fire, expelling heat from the bole (Fernandes and Rigolot, 2007). Resprouting species quickly recover after fire since they are able to keep a part of biomass alive, usually below ground. *Quercus suber* is the only European tree species which is able to resprout from stem buds, protected by the thick bark (cork). Some species invest in post-fire reproduction strategies and, commonly, the recruitment process is stimulated by fire (seed dispersal, germination, or flowering). Obligate-seeders recovery is achieved by germination of fire-resistant seeds, stored in the canopy or in the ground (Lloret, 1998; Arianoutsou and Ne'eman, 2000). *Pinus* species protect their seeds in serotinous cones in the canopy, which respond to fire by rapidly starting seed dispersal in the presence of fire.

However, not all Mediterranean species are adapted to fire (Retana et al., 2002) and, when fires become more severe and frequent, ecosystems may enter in a process of degradation and

desertification. Thresholds in fire severity may determine vegetation survival and ability to recover and, additionally, fire recurrence before trees reach their reproductive maturity may lead to disappearance. If fire becomes too extreme, pine forests may not be able to recover to their previous state (Pérula et al., 2003). The loss of some growth capacity of resprouters after recurrent fires has also been registered (Ferran et al., 1998). This is especially important since recently burned areas seem to be more fire-prone than non-burned areas (Vázquez and Moreno, 2001; Loepfe et al., 2010).

Water availability has a determinant role in primary productivity. Vegetation recovery rates are affected by soil moisture, which is higher in North facing slopes (less exposed to sun radiation and inducing smaller losses by evapotranspiration) and in flat areas or areas with moderate slope, with higher water retention capacity (Tsitsoni, 1997; Pausas et al., 2004; Fox et al., 2008). The precipitation regime has also great influence both on fire risk and in vegetation recovery. Changes in the precipitation regime, such as decreases in rainfall volume and increases in rainfall concentration seem to be occurring in dry, inland areas, where most forests are located (De Luís et al., 2001). Strong and frequent droughts increase water stress during the regeneration process, and more concentrated rainfall volume may intensify erosion and nutrient loss (De Luís et al., 2003), affecting short-term ecosystem development.

Some of the usual erosion prevention and vegetation recovery management practices in the Mediterranean include reforestation or the establishment of seedlings to promote plant re-growth, fragmentation of the landscape and creation of fire break networks to reduce fire propagation, limiting competition and, finally, reduction of dead biomass. Fire-prevention and land management play a determinant role in ecosystems' and territory sustainability but are also crucial to reduce greenhouse gas emissions and accomplish international targets, such as the Kyoto Protocol commitments.

When compared to European Mediterranean countries, Portugal is the country with the highest number of fire occurrences since 1980 and with more burnt area in the last decade (JRC-EC, 2009). According to the DGRF (2008) time-series of burnt area, fires in Portugal show a positive trend both in number and in extension since the 80s and present a high inter-annual variability. Vasconcelos et al. (2001) have shown that in Portugal the large majority of fires are started by human action, accidentally or by arsonists. However, meteorological conditions are also an important factor controlling ignition as well as fire spread (Pyne et al., 1996).

The years of 2003 and 2005 were particularly devastating. The year of 2003 registered the maximal burnt area since 1980, with more than 425000 ha burned (DGRF, 2008), representing about 5% of Portuguese mainland (Trigo et al., 2006); the year of 2005 registered the highest number of fire occurrences since 1980, and the second maximal value of burnt area, with about 338000 ha burnt. The previous maximum for burnt area, circa 182000 ha in 1991, was considerably lower than the area burnt in each of these two years (DGRF, 2008). Pereira et al. (2005) have shown the existence of two main factors controlling the extent of burnt area in Portugal: a relatively long dry period with absence of precipitation in late spring and early summer and the occurrence of very intense dry spells during days of extreme synoptic situations (short term heat waves control). The unprecedented fire events of 2003 and 2005 are, in part, linked to these two main factors. In summer 2003, Europe was stricken by a strong heat wave which also affected Portugal, where the majority of the total area burned was due to large fire events that occurred in the first 15 days of August (Pereira et al., 2005). In 2004/2005, Portugal suffered an exceptional drought, one of the most severe since early 20th century (Garcia-Herrera et al., 2007), that lasted for more than 9 months in more than one third of the country. This severe drought had a strong negative impact in vegetation dynamics, since it was contemporaneous with the period of high photosynthetic activity (Gouveia et al., 2009), and may explain the increased tree mortality during 2005 and 2006 (Catry et al., 2010). Since water availability is a crucial factor in post-fire vegetation recovery, it is worth assessing the impact that these water-stress conditions had on post-fire vegetation recovery.

Land-use occupation in Portugal is dominated by forests, which account for 39% of the total area and are mainly composed by broad-leaved (mostly oaks and eucalyptus) and *Pinus* species, followed by

agriculture, representing 33%, and shrub-land, with 22% (AFN, 2010). According to Nunes et al. (2005), very large fires tend to occur selectively in *Pinus pinaster* forests, followed by eucalyptus or pine/eucalyptus mixed forests and, finally, shrub-land. In fact, *Pinus pinaster* (maritime pine) seems to be facing disappearance risk in many areas, since fire recurrence intervals usually do not allow regenerating pines to reach reproductive maturity (Fernandes and Rigolot, 2007). On the other hand, broad-leaved species seem to regenerate easily and very quickly after fire, since most of them are resprouters and have an established root system and stored energy reserves.

In Portugal, as for many European countries, reforestation of burned areas has been a common technique that carries quite elevated costs. Moreira et al. (2009) have shown that resprouting management as an alternative to reforestation provides better results, with lower costs and several operational advantages. As for the maritime pine, fuel management seems to be more suitable, since it decreases the ecological impact of fire and, hence, tree injury and mortality (Fernandes and Rigolot, 2007). The different response to wildfires and distinct post-fire regeneration strategies of the main species in Portugal require specific management techniques. It is, therefore, crucial to understand post-fire vegetation dynamics and regeneration processes, evaluate how they depend on environmental factors, how long does vegetation take to reach the minimal threshold cover and to recover completely, in order to establish adequate erosion prevention and land management measures.

Post-fire vegetation dynamics may be estimated both by field studies and remote sensing. Remote sensing is a very useful tool, since it enables fire mapping with high resolution as well as the study of vegetation dynamics and stress conditions, at large spatial and temporal scales. It further allows the analysis of isolated regions or with limited accessibility that, otherwise, would be impossible to study. Remote sensing has proven to be a powerful tool to study climatic influence on vegetation dynamics (Vicente-Serrano and Heredia-Laclaustra, 2004; Julien et al., 2006; Karnieli et al., 2006), to assess fire risk (Chuvieco et al., 2010), burn severity and erosion risk (Fox et al., 2008), and to monitor post-fire vegetation recovery (Epting and Verbyla, 2005; Goetz et al., 2006; Minchella et al., 2009).

In order to quantify several aspects of vegetation dynamics based on remote sensing information, vegetation indexes have been derived from satellite measurements of vegetation's reflectance spectrum. The broad-band red and near-infrared channels are the most relevant, since they are related to leaf biochemical constituents (Myneni et al., 1995). Several studies have been conducted in Mediterranean ecosystems in order to test the effectiveness of vegetation indexes in monitoring pre and post-fire vegetation dynamics. The Normalized Difference Vegetation Index (NDVI) has been proven to be adequate to monitor post-fire vegetation recovery (Díaz-Delgado et al., 1998; Díaz-Delgado and Pons, 2001; Hope et al., 2007; Fox et al., 2008; Gouveia et al., 2010), as well as vegetation dynamics and stress conditions, such as drought (Gouveia et al., 2009). The Enhanced Vegetation Index (EVI), which minimizes much of the contamination problems of NDVI, was also used in monitoring spatial and temporal of vegetation cover with satisfactory results (Wittenberg et al., 2007). Spectral Mixture Analysis (SMA) has further been used to derive estimates of green vegetation cover (Röder et al., 2008) and may also be used to discriminate ash from charcoal, thus allowing conclusions about fire severity. This approach seems however to be more appropriate for data recorded with hyper spectral sensors, due to their higher spectral dimensionality (Riaño et al., 2002).

Remote sensing is, thus, a powerful tool since it may be used to obtain information about pre-fire vegetation conditions, burn severity, post-fire vegetation dynamics as well as evaluate the effectiveness of post-fire management actions, in very large areas, with moderate costs.

The main goal of the present work is to evaluate the sensitivity of the mono-parametric model developed by Gouveia et al. (2010) to the time-series length, to missing data and to disturbances in vegetation dynamics, as well as to study vegetation recovery following some of the larger wildfire events that occurred in Portugal over the last decade, through the application of the model to NDVI

data. This study is focused on the 2003, 2004 and 2005 fire seasons since extremely large fire events were registered in those years.

Data characterization and pre-processing are presented in chapter 2. NDVI monthly values, over an 11-years period (1998-2009) and with 1 km spatial resolution, were obtained from VEGETATION dataset and corrected for contaminations such as that by clouds. In order to assess the ecosystems' composition, the Corine Land Cover 2000 (CLC2000) was used. Additionally, a Digital Elevation Model for Continental Portugal was extracted from the GLOBE project dataset.

The methodology follows the procedure used by Gouveia et al. (2010), which is based on spatial cluster analysis and on a mono-parametric vegetation recovery model. Both are described in chapter 3. A cluster analysis was performed on NDVI anomalies over the year following the fire event in order to determine large fire scars for each year. In order to remove phenological variability from the analysis of post-fire vegetation recovery, an ideal annual vegetative cycle was defined and used as a control parameter. The mono-parametric model was then fitted to the observed time-series through a logarithmic regression, which allowed estimation of vegetation recovery rates.

Sensitivity of the mono-parametric model to the starting point was analysed and some corrections introduced in order to ensure the best fit of the model to the observed time-series. As the time-series used in Gouveia et al. (2010) was not long enough to completely cover the vegetation recovery process, the model was validated by applying it to the extended 11-year time-series. Some areas presented diverse problems when the model was applied, thus a correction was introduced, in order to provide a better fit of the regressed curve to the observed time-series. The response of the model to missing data in distinct stages of the recovery process was also evaluated, as well as the effect that disturbances of vegetation dynamics had on model's estimations. The influence of the extreme drought of 2005 on the model's estimations was assessed, being drought defined by the analysis of the NDVI anomaly in a control area near each burnt scar.

In chapter 4, vegetation dynamics is analysed along the 11-year time-series, covering pre-fire and post-fire periods over four fire scars selected from the 2003, 2004 and 2005 fire seasons, located in distinct regions of Continental Portugal. Spatial analysis was performed in order to identify patterns and assess the relevance of driving factors of the recovery process, especially fire damage and pre-fire vegetation density. K-means spatial cluster analysis allowed the identification of relationships between fire damage (estimated by the field of NDVI in May of the year following the fire event), vegetation density (estimated by the median of NDVI over the pre-fire period) and recovery times.

In order to assess differences in the recovery behaviour of the different vegetation types, due to their physical and phenological characteristics, a cluster analysis was performed on recovery time, and land-cover composition of identified clusters was then studied using the Corine Land-Cover 2000 dataset. This analysis allowed the evaluation of distinct behaviours for different vegetation types and revealed the existence of recovery patterns.

The influence of terrain characteristics, particularly slope aspect and altitude on the regeneration process was finally evaluated. Slope was evaluated by calculating the gradient of the digital elevation map, in the North-South and West-East directions. However, only the Northern and Southern slope aspects were considered in the analysis since they present more pronounced contrasts in sun radiation and, thus, in soil moisture content.

Chapter 5, the final chapter, contains a summary of results obtained and an overview of the most important conclusions.

2. Data and Pre-Processing

2.1 Normalized Difference Vegetation Index

Remote sensing is a powerful tool in the analysis of vegetation activity, since it allows the detection of vegetation and the assessment of the evolution of its status and, therefore, to verify and analyse temporal changes in vegetation cover and behaviour.

Satellite detection of vegetation is related to the biochemical activity of light absorbers that are responsible for photosynthesis and enables the monitoring of vegetation density and vitality. The fact that the chlorophyll absorption maximum is at about 0.69 μm (RED), while reflectance in the near-infrared region (NIR, 0.85 μm) is very high (Myneni et al., 1995) allows distinguishing vegetation from bare soil, snow cover or water whose reflectance spectra are quite different, as shown in Fig. 1.

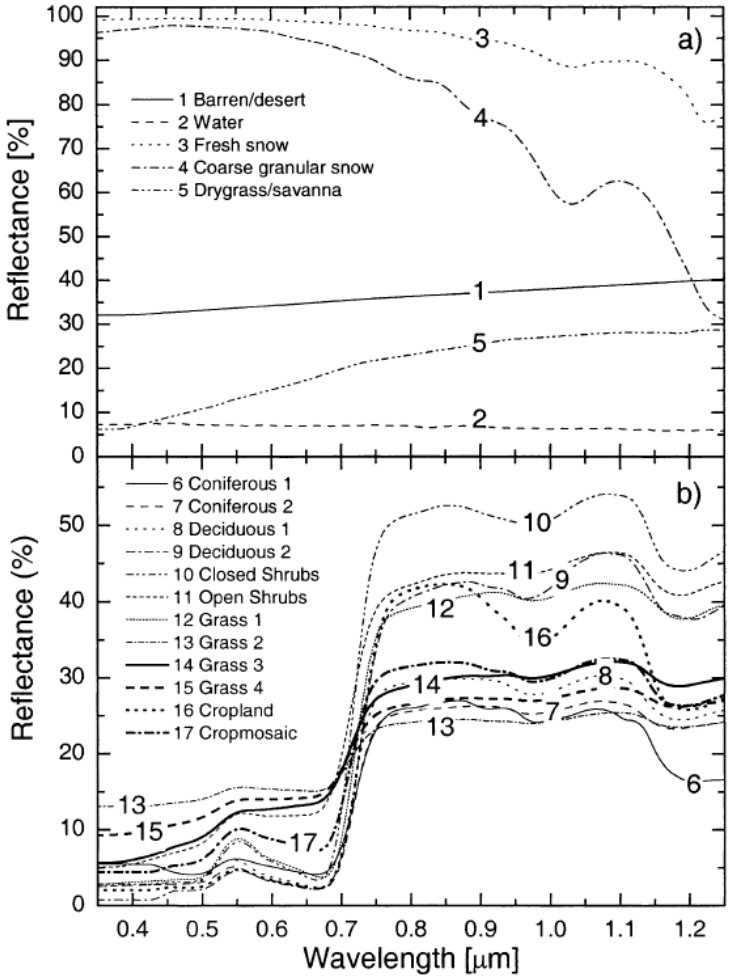

Fig. 1 – Normalized reflectance spectra for several non-vegetated areas (panel a) and for different types of vegetated land-cover (panel b) (Myneni et al., 1995).

Vegetation indexes have been derived from this profile, where the contrast between red and near-infrared reflectance is particularly important. Several authors have shown that vegetation indexes provide a good estimation of the vegetation amount (Tucker et. al., 1979), fraction of absorbed photosynthetically active radiation (Asrar et al., 1984) and unstressed vegetation conductance and photosynthetic capacity (Sellers et al., 1992).

Proposed by Rouse et al. (1974), the NDVI is commonly used in vegetation cover assessment. It is defined as:

$$NDVI = \frac{\rho_{nir} - \rho_{red}}{\rho_{nir} + \rho_{red}} \quad (1)$$

where ρ_{nir} is surface reflectance on Near Infra-Red channel and ρ_{red} corresponds to surface reflectance on Red channel.

NDVI values for green vegetation typically range from 0.2 to 0.8, whereas those for snow, bare soil or rocks range from -0.2 to 0.1. Vegetation under stress conditions or dead biomass is also characterized by low values of NDVI, since reflectance in the NIR band decreases considerably. Therefore, NDVI provides a simple tool to discriminate vegetation from other land-cover types and to determine the healthiness of biomass. However, NDVI satellite measurements are affected by atmospheric effects, suffering diverse contamination problems from clouds or aerosols, by soil reflectance and, also, by geometrical and radiometric effects. As these problems may mislead the analysis, it is very important that most of the perturbations are removed in order to obtain information with satisfactory degree of accuracy. More complex indexes have been developed to minimize contamination effects, such as the Soil Adjusted Vegetation Index (Huete, 1988) or the Atmospherically Resistant Vegetation Index (Kaufman and Tanré, 1992).

In spite of some contamination problems, which demand correction procedures, NDVI has been widely used due to its simplicity and low computational cost as well as to the availability of continuous time-series in relatively long periods (29 years of AVHRR-NDVI and 11 years of VEGETATION). NDVI has been used to assess climate influence in vegetation dynamics with satisfactory results (Vicente-Serrano and Heredia-Laclaustra, 2004; Julien et al., 2006, Gouveia et al., 2008).

2.2 NDVI Data and pre-processement

In the present work, vegetation dynamics is assessed using corrected NDVI datasets as acquired from the VEGETATION instrument on board of SPOT4 and SPOT5 satellites. Since 1998, the VEGETATION instrument has been providing high quality global monitoring on a daily basis of land-cover dynamics, in the Blue (B0, 460 nm), Red (B2, 670 nm), Near Infra-Red (B3, 840 nm) and Medium Infra-Red (MIR, 1640 nm) spectral bands (Hagolle et al., 2005). NDVI data were extracted from S10 products of VITO database (http://free.vgt.vito.be), which provides a 10-day synthesis of the daily products, based on the Maximum Value Composite method (MVC). This method consists in selecting the highest value of NDVI for each 10-day period for each pixel, a procedure that removes most of the cloudy pixels (Holben, 1986). MVC-NDVI are also corrected for atmospheric effects, using a modified version of the Simple Method for the Atmospheric Correction (SMAC) code, which accounts for absorption and scattering processes (Rahman and Dedieu, 1994). Both geometric and radiometric corrections are performed, the latter using a linear model that normalizes Charge-Coupled Device response (Maisongrande et al., 2004). S10 MVC-NDVI values are supplied on a regular latitude-longitude grid, using the WSG84 ellipsoid, at the resolution of 0.008928º (approximately 1km^2 over the Equator).

MVC-NDVI data for Portugal were selected for a region extending from 37ºN to 42ºN and from 10ºW to 6ºW within a period ranging from September 1998 to August 2009. Despite the corrections described previously, MVC-NDVI data still present problems related to cloud contamination, snow cover, shadows, directional response dependence of the spectral response or phenological spatial and temporal variability. Therefore, each annual time-series of MVC-NDVI was analysed and corrected following the procedure applied by Stökly and Vidale (2004) to the Pathfinder NDVI data in order to create a continuous European vegetation phenology dataset at 10-day temporal and 0.1º resolution. This procedure comprises a spatial interpolation to replace processing artefacts and no-data values in the dataset and the adjustment of NDVI time-series by using a temporal interpolation. This is

performed by applying an adjustment algorithm based on a weighted second-order Fourier analysis, as described by Sellers et al. (1997) and Los (1998), in order to create an European Fourier-Adjusted and Interpolated (EFAI) NDVI dataset. Different weighting functions are assigned to vegetation with a continuous transition between growing and non-growing periods, such as evergreen, and for vegetation with a marked vegetative cycle between dormant and active periods. Therefore, the definition of the growing season is required, which in Portugal coincides with the hydrological year, starting in the second decade of August from the previous year, and ending in the first decade of August from the hydrological year considered. Time series of MVC-NDVI and EFAI-NDVI for the 2001 hydrological year are presented in Fig. 2 (black dots and red lines, respectively), and the time series of EFAI-NDVI for 1999-2009 time-series is presented in Fig. 3, averaged over areas with different land-cover. Distinct phenologies between broad-leaved and mixed forest (low intra-annual variation) and arable land are clear, the latter with a marked vegetative cycle. Also, the effects of droughts on plant phenology are visible, especially for the years of 1999 and 2005.

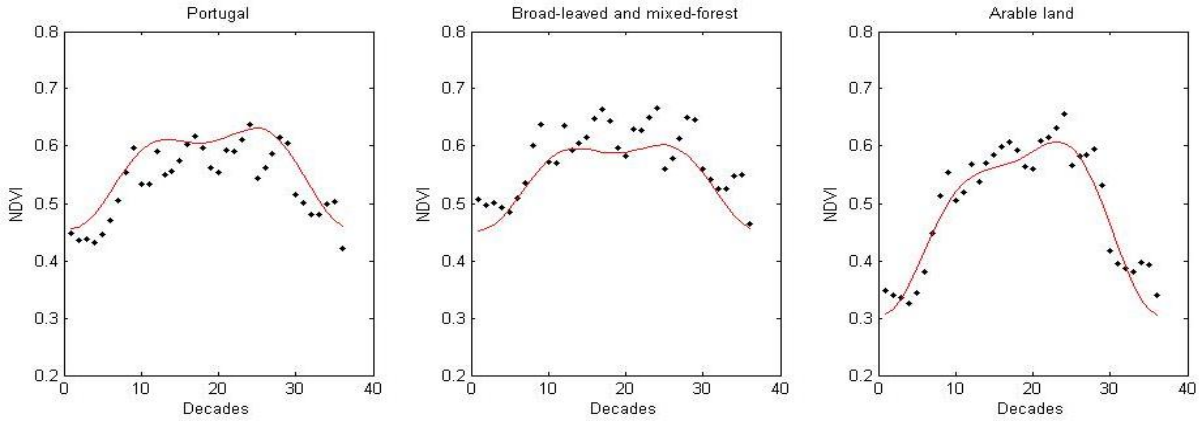

Fig. 2 – MVC-NDVI (black dots) and the fitted EFAI-NDVI time series (red line) for the hydrological year of 2001, averaged over Continental Portugal for all pixels (left panel), broad-leaved and mixed forest pixels (central panel) and pixels of arable land (right panel).

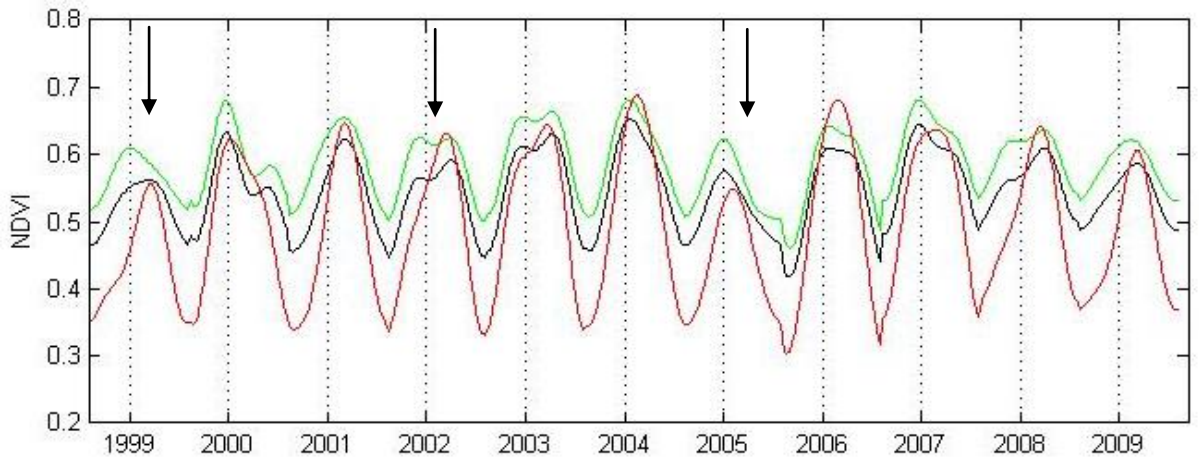

Fig. 3 – EFAI-NDVI time-series averaged over Continental Portugal for all pixels (black line), for pixels of broad-leaved and mixed forest (green line) and for pixels of arable land (red line). Time-series starts on the second decade of August 1998 and ends on the first decade of August 2009. Vertical dotted lines indicate the month of January for each year. Black arrows point the drought episodes of 1999, 2002 and 2005.

2.3 Land-cover data

Land-cover data were extracted from Corine Land-Cover 2000 (CLC2000) project, which provides quantitative and qualitative information on land-cover, over the majority of European territory. Since the first Corine Land-cover database was released in 1990 (CLC1990), Corine Land-Cover also provides valuable information on land-cover changes. This database is organized according to a hierarchic nomenclature in 3 levels. The third level includes 44 classes, providing detailed information on agriculture regimes and forest main species. CLC2000 was used instead of Corine Land-Cover 2006 (which was available) because the work is focused on fires which occurred during the period from 2003 to 2005.

In Portugal, the CLC2000 map was developed by Instituto Superior de Estatística e Gestão da Informação (ISEGI).The CLC2000 raster map for Portugal is provided at 250m spatial resolution, using a Transverse Mercator projection with the Hayford spheroid (Fig. 4).

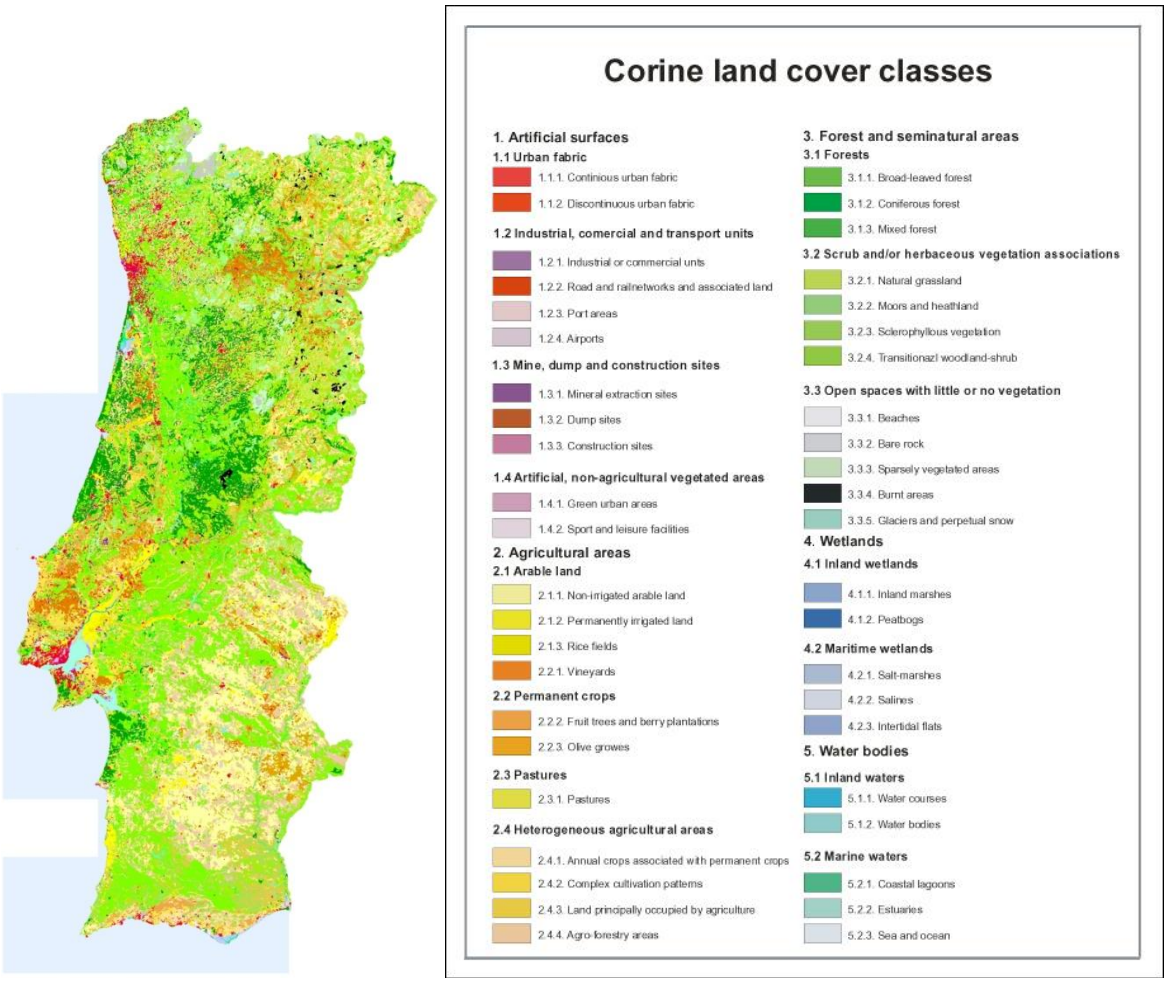

Fig. 4 – Corine Land-cover 2000 map for Continental Portugal as developed by ISEG at 250m spatial resolution (left) and land-cover classes and nomenclature (right).

Remote sensing data used in this work is in geographic coordinates and at 1km resolution, therefore, CLC2000 map was degraded to the resolution of 1km according to the commonly used majority rule (Turner et al., 1989).

2.4 Digital elevation model

Several studies indicate that post-fire vegetation recovery may be affected by terrain, namely by altitude, slope or aspect (Pausas and Vallejo, 1999; Pausas et al., 2004; Wittenberg et al., 2007). A Digital Elevation Model (DEM) was used to determine terrain characteristics. The model was provided by the Globe Land One-kilometre Base Elevation (GLOBE), version 1.0, and is defined in a regular grid in latitude-longitude coordinates in the WSG84 ellipsoid, at spatial resolution of 30 arc-seconds (0.00833º). Vertical units represent elevation in meters above the mean sea level and have variable accuracy, depending on the sources from which they are derived (Hastings et al., 1999). DEM data for Portugal were selected for a region extending from 37ºN to 42ºN and from 10ºW to 6ºW. A triangle based linear interpolation was used to fit DEM data coordinates into MVC-NDVI coordinates. DEM map for Continental Portugal used in this work is shown in Fig. 5.

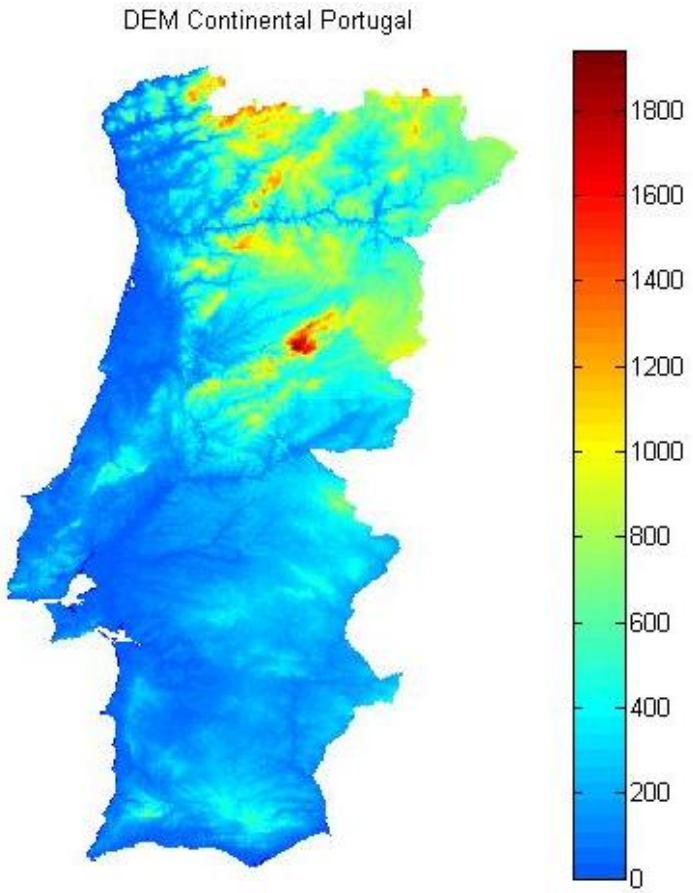

Fig. 5 – Digital Elevation Model for Continental Portugal at 1km spatial resolution, corrected to fit MVC-NDVI data coordinates. Vertical units represent elevation in meters above mean sea level.

3. Vegetation recovery

Detection of large fire scars and analysis of vegetation recovery follows the procedure in Gouveia et al. (2010), which is mainly divided in three categories:

a) Spatial analysis of the data to identify burnt areas;

b) Fit of a mono-parametric model of post-fire vegetation recovery to estimate post-fire vegetation recovery times;

c) Analysis of spatial distributions of post-fire vegetation recovery times to assess the roles of pre-fire vegetation density and of fire damage.

3.1 Burnt areas identification

Fire scars were spotted through a cluster analysis of monthly MVC-NDVI anomalies. The analysis was carried out over each hydrological year, defined as the period ranging from September of that year to August of the following year. Each monthly NDVI anomaly was defined as the departure of NDVI value of a given month to the median of the NDVI for that month, computed over the considered period (1998-2009). Median value was used instead of the mean in order to minimize the bias effect of extremely low NDVI values attained in drought years (Gouveia et al., 2009). Unsupervised clustering of the spatial distribution of monthly NDVI anomalies was performed based on the K-means partition clustering method (MacQueen, 1967; Hartigan and Wong, 1979). This algorithm relies on an iterative refinement technique that minimizes the sum of squares of distances between data and the cluster centroid. By recalculating the centroids until distances reach the minimal value, this method allows an optimally compact and separated set of clusters. Large burnt scars are associated with extremely low values of NDVI anomaly, that persist throughout the vegetative cycle of the following year. Therefore, a cluster analysis of spatial distribution of NDVI anomalies performed in the year following each fire season allows the identification of large fire scars.

The present work focuses on fires which occurred in the 2003, 2004 and 2005 fire seasons. Large fires that occurred in 2003 were identified via cluster analysis of the NDVI anomalies over the hydrological year of 2004. As shown in Fig. 6, two clusters were identified, whose centroids clearly show distinct behaviour over the 2004 hydrological year.

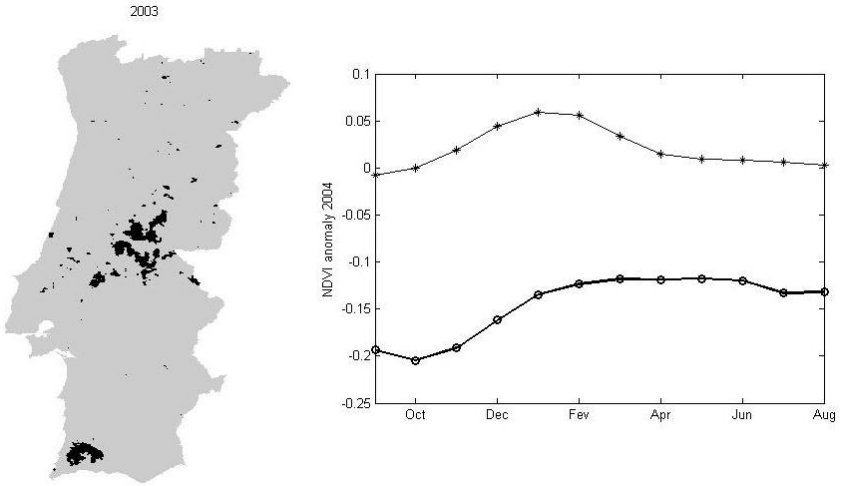

Fig. 6 – Burnt areas (black pixels) in Continental Portugal during the 2003 fire season (left panel), as identified by a cluster analysis of MVC-NDVI anomalies throughout the 2004 hydrological year (right panel). Time series of two identified centroids of identified, associated to burnt pixels (bold line with open circles) and to non-burnt pixels (black asterisks).

One of the centroids (open circles, bold line) is characterized by large negative values of NDVI monthly anomaly, especially in the first months of the hydrological year, whilst the other (black

asterisks) is described by lower, and mainly positive, values of monthly anomalies. The spatial distribution of the centroid with persistently negative anomalies in the year following the fire season indicates burnt scars and matches the results obtained by Gouveia et al. (2010).

The same analysis of NDVI anomalies was performed for 2005 and 2006 hydrological years with the aim of spotting the large burnt areas of 2004 and 2005 fire seasons (Figs. 7 and 8).

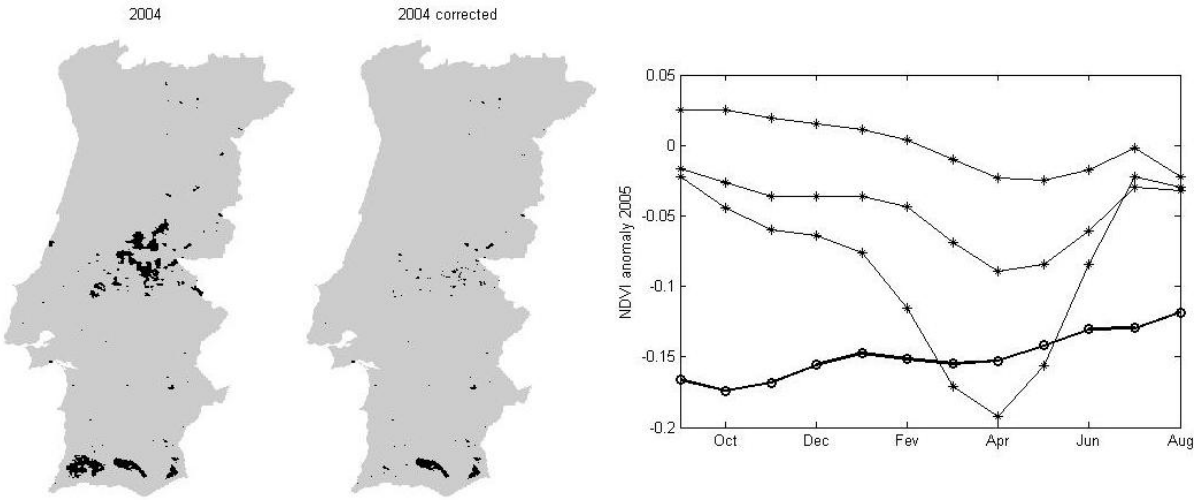

Fig. 7 – Burnt areas (black pixels) in Continental Portugal during the 2004 fire season as identified by cluster analysis (left panel) and corrected by removing pixels from the fires of 2003 fire season (centre panel. Cluster analysis was performed on MVC-NDVI anomalies throughout the 2005 hydrological year (right panel). Four clusters were identified, being the one with centroid with large negative values in the first months associated to burnt pixels (bold line with open circles), and the others to non-burnt pixels (black asterisks).

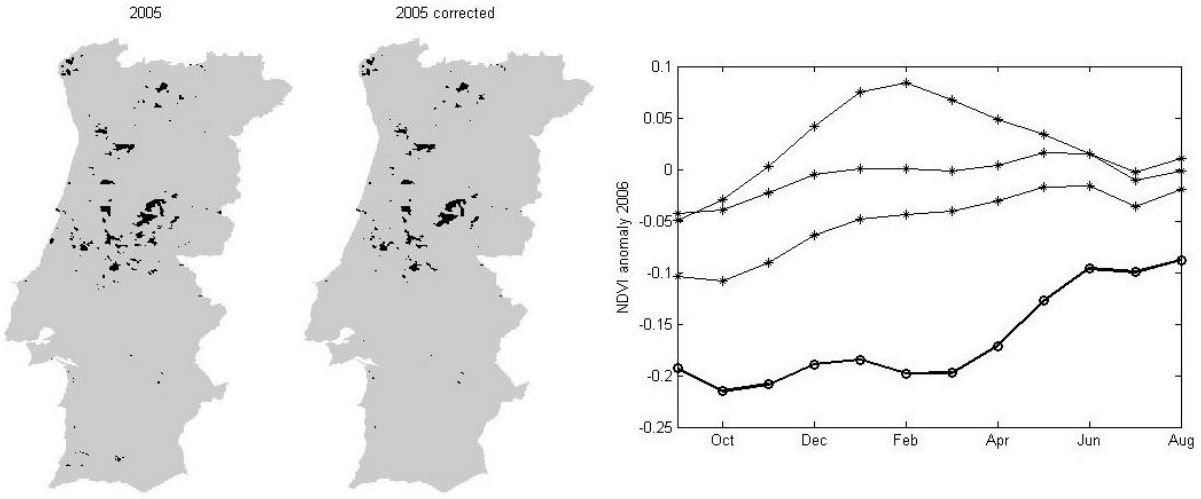

Fig. 8 – As in Fig. 7 but respecting to the 2005 fire season. Four clusters were identified, being the one with centroid with large negative values in the first months associated to burnt pixels (bold line with open circles), and the others to non-burnt pixels (black asterisks).

Cluster analysis for 2004 fire season allowed the identification of four clusters whose centroids are associated with burnt pixels (open circles, bold line), and non-burnt pixels (black asterisks). The two clusters, with centroids with very low values of anomaly especially from January until June, seem to be associated to pixels moderately or severely affected by the 2005 drought. The analysis for the 2005

fire season is quite similar, with four clusters being identified, associated with burnt areas (open circles) and with non-burnt areas (black asterisks). Clusters with negative anomaly values, especially in the last months of 2005, seem to correspond to areas affected by the 2005 drought or to scars recovering from previous fires. However, in both cases, contamination from previous fires was registered, since some burnt pixels kept very low values of NDVI anomaly for more than one year after the fire. This is especially the case of pixels corresponding to the scars from fire events occurred in 2003, whose recovery was severely affected by drought. Pixels from previous fires seasons were removed from the 2004 and 2005 spatial analysis, as shown in Figs. 7 and 8 (central panels).

Obtained burnt areas for the analysed fire seasons were compared to maps of burnt scars provided by AFN, which are based on end-of-fire-season Landsat (2000-2004) and Modis (2005) imagery (Fig. 9). It is apparent that pixels belonging to the clusters associated with strong negative NDVI anomalies over the year following the fire occurrence, after the removal of contamination from previous fires, match the large burnt areas spotted by AFN. Although smaller fire scars are not spotted by this method, the procedure seems to be suitable for the identification of large burnt areas in the three years considered.

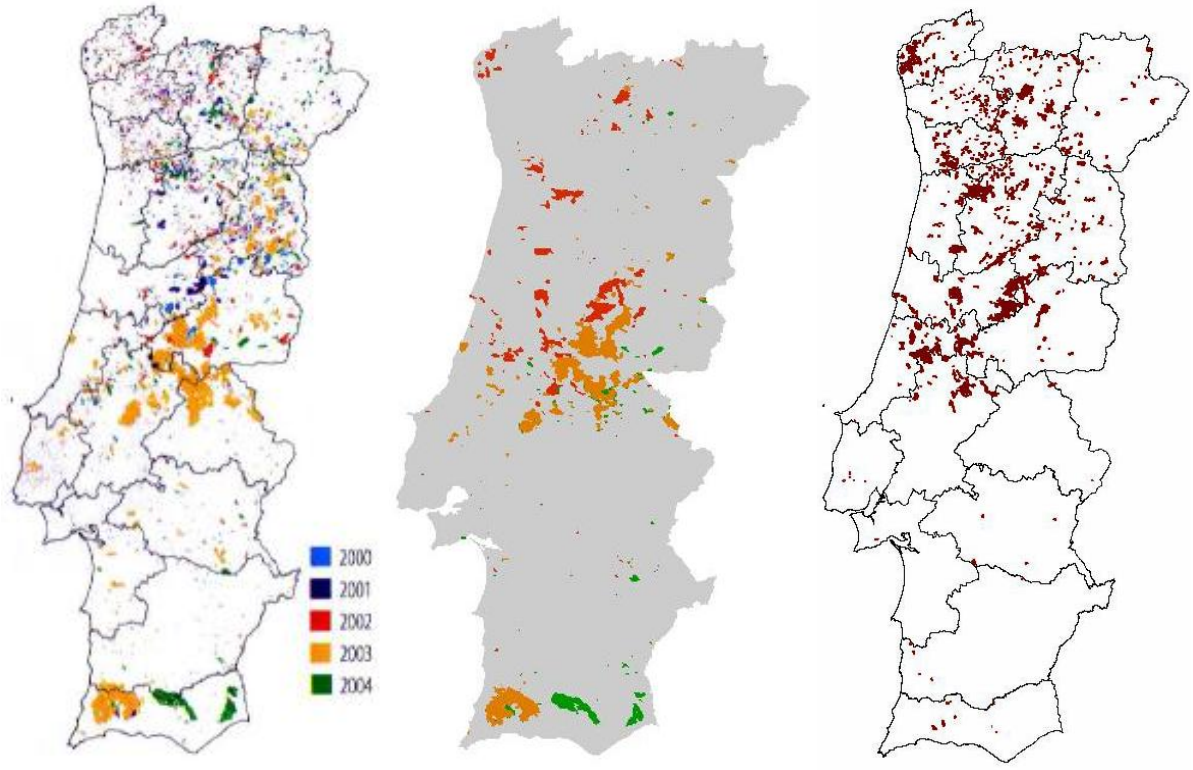

Fig. 9 – Burnt areas in Continental Portugal for the 2000-2004 period as identified by AFN, based on Landsat imagery (left panel). Burnt areas in Continental Portugal for the 2003 (orange pixels), 2004 (green pixels) and 2005 (red pixels) fire seasons as obtained by the cluster analysis of the NDVI anomalies over the year following each fire season (central panel). Burnt areas in Continental Portugal for 2005 as identified by AFN, based on Modis imagery (right panel).

As shown in Fig. 10, several burnt scars from 2003, 2004 and 2005 fire seasons were selected, covering different geographical locations in Continental Portugal and presenting distinct vegetation composition. Regions I to IV correspond to fires from 2003 fires season, Regions V and VI to 2004 and Regions VII to IX to 2005.

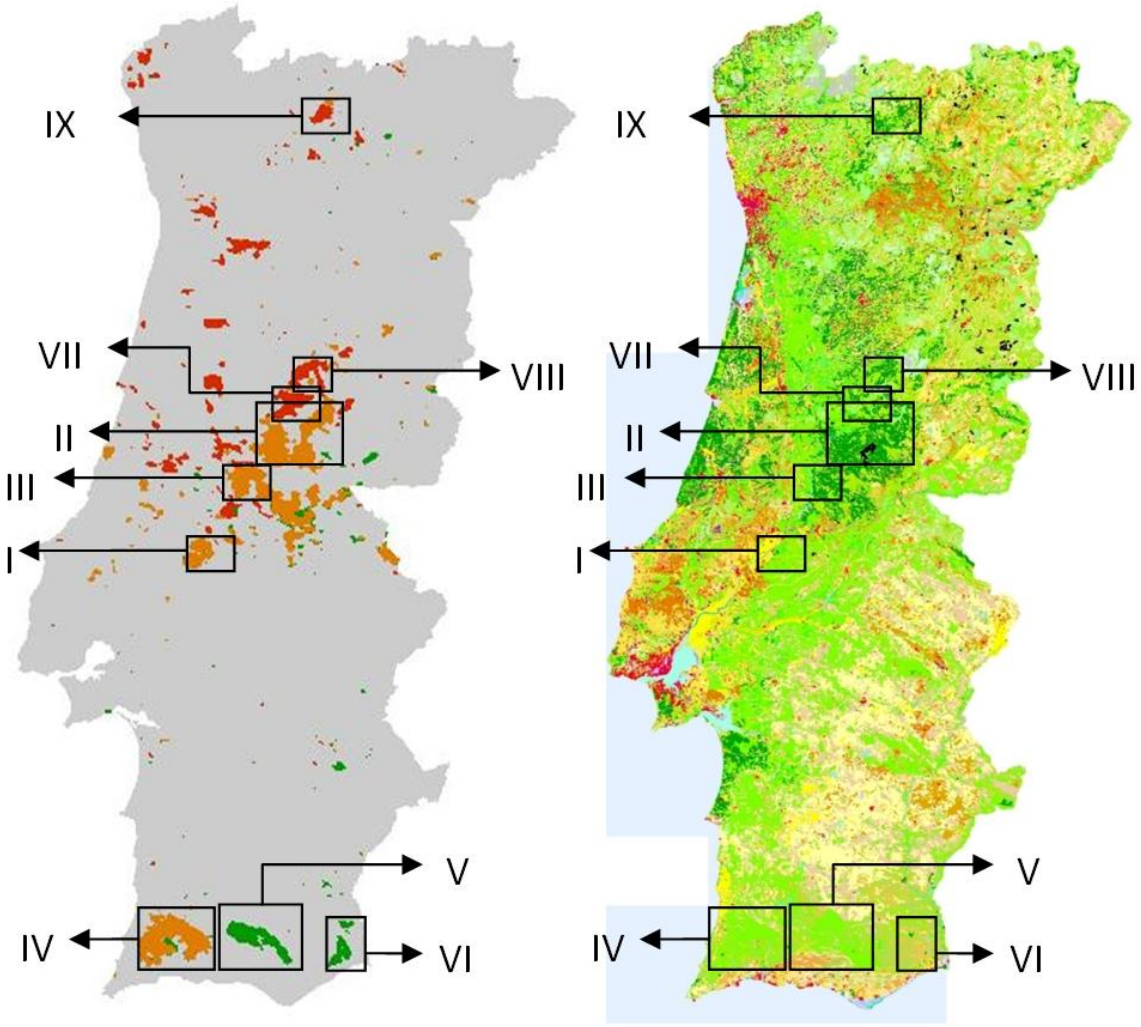

Fig. 10 - Burnt areas in Continental Portugal for the 2003 (orange pixels), 2004 (green pixels) and 2005 (red pixels) fire seasons as obtained by the cluster analysis of the NDVI anomalies over the year following each fire season (left panel). Corine Land-cover 2000 map for Continental Portugal developed by ISEG at 250m spatial resolution (right panel). Selected areas for the present work are identified by labels associated to rectangular frames.

3.2 Model of post-fire vegetation recovery

Several studies have been conducted in order to quantitatively analyse vegetation regeneration followingr fire events (Díaz-Delgado et al., 1998; Díaz-Delgado and Pons, 2001; Röder et al., 2008). Díaz-Delgado et al. (1998) have used spatial averages of Landsat MSS NDVI values over the burnt area for a 19 year period to calculate vegetation recovery rates. Control areas near the burnt sites (with similar phenology and composition) were chosen and the ratio between NDVI values for the burnt and control areas was computed, in order to eliminate phenological variability. A logarithmic regression model was fitted to the time-series, which successfully enabled the estimation and comparison of recovery rates for areas with different vegetation composition. Gouveia et al. (2010) proposed a method to estimate vegetation recovery rates which has the advantage of using solely data from the burnt area, avoiding the definition of control plots (which may be inexistent or inadequate in certain situations). This method is used in the present work to analyse post-fire vegetation dynamics, based on NDVI data, and is next described as in Gouveia et al. (2010).

The model makes use of an asymptotic annual cycle that describes an ideally healthy state of vegetation, along the vegetative cycle. Such ideal state, NDVI*(t), is a periodic function with period of one year. For a given location, vegetation greenness at time t is given by NDVI(t) and the corresponding lack of greenness, $y(t)$ is defined as:

$$y(t) = NDVI(t) - NDVI^*(t) \tag{2}$$

Instantaneous vegetation recovery rate (dy/dt) is assumed to be proportional to the lack of greenness, that is

$$\frac{dy(t)}{dt} = -by \tag{3}$$

where b is a positive constant, the minus sign indicating that vegetation recovery rate is a positive quantity (since $y(t)$ is negative until vegetation recovers completely). After integrating the previous ordinary differential equation, lack of greenness is given by

$$y(t) = ae^{-bt} \tag{4}$$

where a=NDVI(t=0)-NDVI*(t=0) is a negative constant that represents the lack of greenness at the time of occurrence of the fire episode and b is the recovery rate. Since a corresponds to the largest negative value of lack of greenness, it may be also used as an indicator of fire damage. This model is similar to others used in environmental science, like biological oxygen demand (BOD) evolution in polluted water (Sawyer et al., 2002).

In order to estimate vegetation recovery rate (b), the remaining parameters, NDVI* and a, must be determined. NDVI* was estimated via an annual ideal vegetative cycle (the so-called Gorgeous Year, GY) given by the maximum of NDVI for each month over the pre-fire period. Parameter a was simply set as the observed monthly NDVI value of the month immediately following the fire occurrence (t=0). Since monthly mean values of 10-day composites of NDVI are used, NDVI values in the month of the fire are contaminated by NDVI values before the fire event and, hence, fire damage is correctly estimatedafter the month of the fire occurrence.

The value of b may then be estimated by means of a regression analysis of the following linear expression, which is equivalent to Eq (4)

$$\ln\left[\frac{y(t)}{a}\right] = -bt \tag{5}$$

where

$$\begin{aligned} y(t) &= NDVI(t) - GY(t) \\ a &= y(t=0) = NDVI(t) - GY(t) \end{aligned} \tag{6}$$

It is worth noting that GY plays the same role as the one played by control areas in other works (Díaz-Delgado et al., 1998, 2003), since it eliminates phenology dependency of post-fire vegetation dynamics. Vegetation recovery time is defined as the period required for spatially averaged lack of greenness over each area to reach 90% of the mean value over the pre-fire period.

Figure 11 presents MVC-NDVI time-series (grey curves) and respective GY (black curves). The values were spatially averaged over Regions I and II, as in Gouveia et al. (2010). In Fig. 12 the time series of lack of greenness, y is shown, as well as the modelled curve and respective limits of the 95%

confidence intervals, as in Gouveia et al. (2010). It is worth noting that their time-series was not long enough to observe vegetation recovery, which is indicated by vertical arrows in Fig. 12. It may be noted that the two regions studied in Gouveia et al. (2010) correspond to Regions II and IV in the present work and will be analysed further.

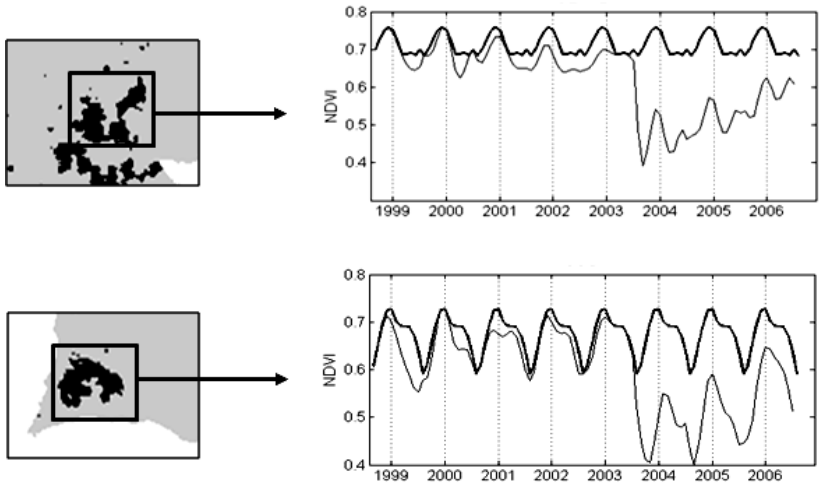

Fig. 11 – Time series of NDVI (grey curves) spatially averaged over the two selected large fire scars respectively located in Region I (upper panel) and in Region II (lower panel). Black curves represent the Gorgeous Years (GY) of vegetation, given by the annual cycles of maximum NDVI for each month over the considered period. Vertical dotted lines indicate the month of January for each year. (Gouveia et al. 2010)

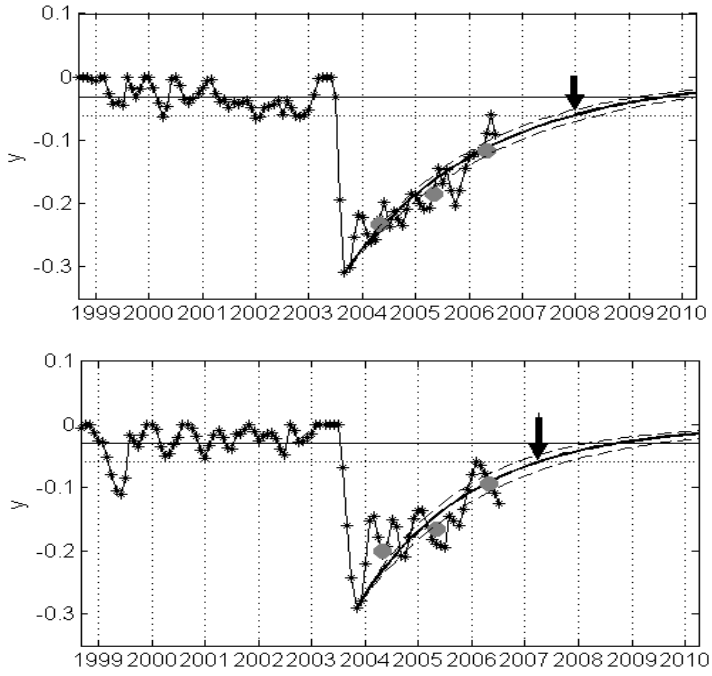

Fig. 12– Time series of observed (lines with asterisks) and modelled (bold curves) values of monthly values of lack of greenness, *y*, over the large fire scars located in Region 1 (upper panel) and in Region II (lower panel). The dashed curves indicate the 95% confidence limits of the regressed curve and the large grey circles indicate the annual means of *y*. The horizontal dotted line represents the level of vegetation recovery defined as 90% of the mean value of *y* during the pre fire period (represented, in turn, by the horizontal solid line). Arrows indicate the estimated recovery dates, defined as the instant when the modelled curves of *y* cross the level of vegetation recovery. Vertical dotted lines indicate the month of January for each year. (Gouveia et al. 2010)

3.2.1 Adjustment to the starting point

Parameter *a*, i.e. the lack of greenness in *t*=0, was set as the first month immediately after the month of the fire event. However, this approach did not seem suitable for all situations since sometimes the minimal value of the lack of greenness was not reached in the month immediately after the fire, but two or more months later, as it may be observed in Region VI (Fig. 13). This is due to the fact that a considerable part of the biomass severely affected by fire may survive in the first months, but hardly resists to the adverse conditions during autumn and winter that follows, such as intense cold and heavy rainstorms.

The starting point for vegetation recovery must be chosen cautiously and it seems reasonable to assume that the regeneration process begins only right after the minimal vegetation cover is reached, within a period ranging from the beginning of the fire season of each year to the beginning of the fire season of the following year. Parameter *a* (*y(t=0)*) was therefore set by choosing the month corresponding to the minimal value of the lack of greenness (*y(t)*) over a period ranging from April, the beginning of the fire season, of each year until March of the following year. As shown in Fig. 13, this approach provided a better adjustment of the model to the observed values, especially to the first months of recovery, leading to considerable differences in recovery times accompanied by a reduction of the extension of the 95% confidence intervals.

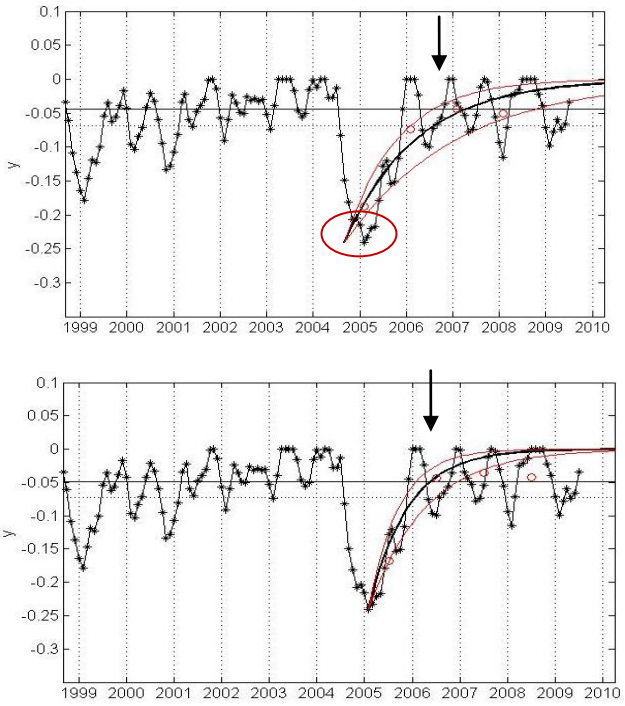

Fig. 13 – Time-series of observed (black line with asterisks) and modelled (black line) *y* time-series averaged over the burnt scar in Region VI without correction (top right panel) and corrected (bottom right panel). Red ellipse (upper right panel) highlights the misadjustment of the uncorrected modelled curve vegetation recovery. Vertical arrows indicate vegetation recovery.

Estimated vegetation recovery times and respective 95% confidence intervals are 25, [19, 38] months for uncorrected modelling and 13, [10, 18] months for corrected modelling. This adjustment procedure was tested for several burnt areas of the three fire seasons considered leading to satisfactory results.

It is worth stressing that small differences (one or two months) in the starting point may lead to substantial variations (several months) in estimated recovery times, as it would be expected given the exponential character of the model. Moreover, the adjustment of the starting point of the modelled time-series to the minimal value of observed lack of greenness between two fire seasons generally led to narrower 95% confidence intervals. Therefore, use will be made of this adjustment procedure.

3.2.2 Application of the model to an extended dataset

The model of post-fire vegetation recovery was applied in Gouveia et al. (2010) to an 8-year time-series which was not long enough to observe complete recovery of vegetation in burnt scars, as mentioned previously. The present work relies on a longer time-series, covering 11 years, which allows the observation of vegetation recovery in the burnt scars analysed in Gouveia et al. (2010), identified in this work as Regions II and IV, respectively. A preliminary validation of the model is, thus, possible and is crucial for the correct implementation of the model.

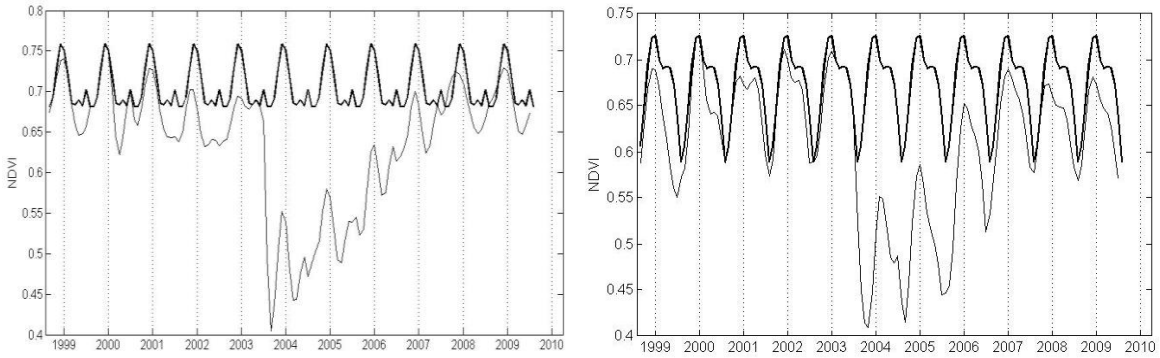

Fig. 14– Time series of NDVI (grey curve) and of GY (black curve) spatially averaged over Region II (left panel), and Region IV (right panel).

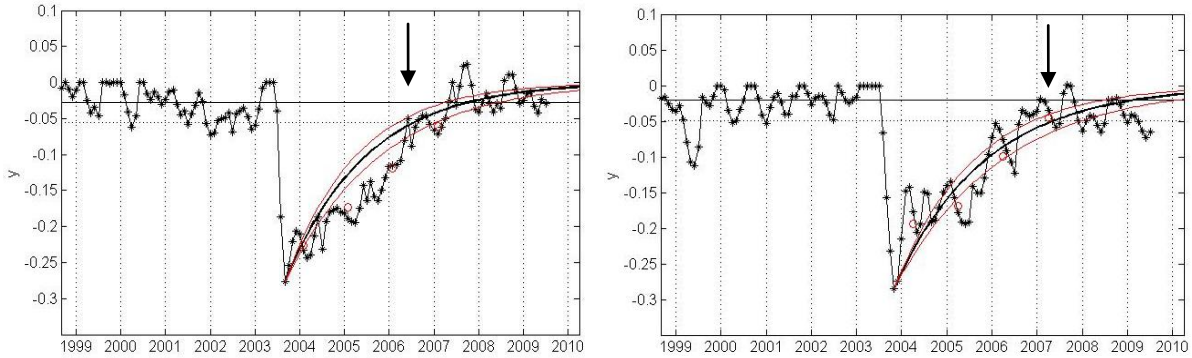

Fig. 15 – Lack of greenness, *y,* time-series (black line with asterisks) and modelled curve (solid line) of vegetation recovery, spatially averaged over Region II (left panel) and Region IV (right panel).

Fig. 14 presents monthly values of MVC-NDVI and GY for Regions II and IV, whose respective *y* time-series and modelled curves are shown in Fig. 15. Estimated vegetation recovery time for Region II is 36 months, as indicated by the vertical arrow. This result is substantially different of the estimated 52 months of recovery time with 95% confidence interval of [48, 59] provided by the application of the model to a shorter time series (8 years) over the same region by Gouveia et al. (2010), as shown in Fig 12. For Region IV, estimated recovery time is 44 months, which differs by only one month of the estimated 43 months in Gouveia et al. (2010), and is within the respective 95% confidence interval of [38, 49] months.

In Region II, the regressed curve for *y* over the 11-year time-series seems to have been pushed by the positive values of some points within the post-fire period. The existence of several points corresponding to higher levels of vegetation activity than before the fire occurrence is not consistent with the definition of GY. A careful observation of the NDVI time-series (Fig. 14) seems to reveal a change in the vegetative cycle over the post-fire period, especially after 2007. It is worth noting that maximal NDVI values reached over the vegetative cycle following recovery, especially from 2007 onwards, are lower than before the fire. The presence of several positive values of *y* is justified by a shift in the beginning of the growing season. In fact, vegetation dynamics after 2007 seems to correspond to a distinct vegetative cycle, as the growing season starts earlier, and the second peak of

the vegetative cycle completely disappears. This apparent transformation of the vegetative cycle may be due to changes in the ecosystem's composition, however this cannot be evaluated using this method since NDVI does not provide any sort of information about ecosystem's composition or structure. Although high values of NDVI generally indicate higher levels of vegetation cover, it does not seem correct to consider then in this analysis, since they may introduce unrealistic phenological variability. It is, therefore, more appropriate to remove from the regression analysis those pixels corresponding to distinct vegetation behaviour.

The model of post-fire vegetation recovery was applied to Regions I to IX over distinct periods: (i) from September 1998 to August 2006, corresponding to the time-series in Gouveia et al. (2010); (ii) from September 1998 to August 2009, corresponding to the complete time-series; (iii) the complete time-series excluding all the months following the first month with positive *y*, if there are two or more months with positive *y*. The criterion in (iii) was defined in order to disregard cases of a single month presenting positive *y*, since it does not imply a modification of the vegetative cycle.

Fig. 16 presents the *y* time-series corresponding to these criteria as well as the respective modelled curves for Regions II and IV.

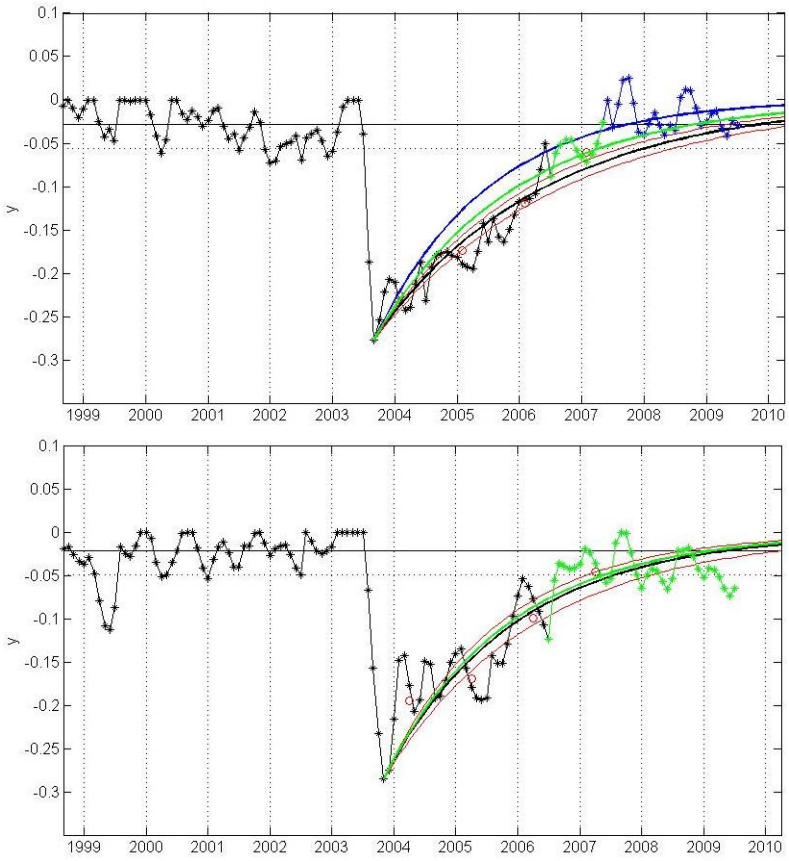

Fig. 16 – As in Fig. 15 but respecting to Region II (top panel) and Region IV (bottom panel) for distinct periods corresponding to criteria (i) (black), (ii) (blue) and (iii) (green). Red lines indicate 95% confidence limits of the regressed curve (i). For GII, *y* time-series and modeled curves (ii) and (iii) are coincident.

Estimated recovery times respecting to criterion (i) are slightly different from the results in Gouveia et al. (2010), i.e. 54 months for Region II and 46 months for Region IV. These differences are due to small changes of NDVI between the two versions of the datasets that were used here and in Gouveia et al. (2010). Observation of *y* time-series of Region II over the 11 years (blue) indicates that positive values of *y* have a strong positive influence on the modelled curve, which is markedly far from observed *y* values in the first years of recovery and from the 95% confidence limits of the regressed

curve of (i), leading to a substantially shorter estimated recovery time. The modelled curve corresponding to the criterion (iii) seems to provide a better adjustment to observed *y* values during the regeneration period, despite lying outside the 95% confidence limits of the regressed curve of (i). For Region IV, modelled curves (ii) and (iii) coincide since there is only one positive value of *y* observed in the post-fire period. The existence of one month with positive *y* (due to a moderately high NDVI value in the period of lower activity in the vegetative cycle and not to an extremely high NDVI value) does not seem to affect the regression analysis. In fact, there does not seem either to be any change in the vegetative cycle characteristics.

Obtained estimates of recovery times for each criterion and for all regions (Table 1) indicate that, for most areas, the modelled fit for criterion (i) provided a satisfactory assessment of vegetation recovery time. Recovery times estimated using criteria (ii) and (iii) for burnt scars in Regions IV, V, VI, VIII and IX belong to the 95% confidence intervals using time-series (i) and differ only by six months or less. It is worth stressing that for Regions VIII and IX the time-series in (i) covered only the first year following the fire occurrence and therefore the criterion was not applied to them. The other four Regions present significant differences in estimated recovery times, which must be understood.

Table 1 – Estimates (t_R) and 95% confidence intervals ($I_{95}[t_R]$) of recovery time respecting to the fit by linear regression of the mono-parametric model of vegetation recover using criteria (i), (ii) and (iii, in all selected Regions.

	(i)		**(ii)**		**(iii)**	
	t_R (months)	**$I_{95}[t_R]$ (months)**	**t_R (months)**	**$I_{95}[t_R]$ (months)**	**t_R (months)**	**$I_{95}[t_R]$ (months)**
Region I	51	[44, 61]	65	[61,71]	65	[61,71]
Region II	54	[49, 59]	36	[32,42]	45	[42, 49]
Region III	58	[53, 65]	44	[38, 52]	42	[38, 46]
Region IV	46	[41, 53]	44	[39, 52]	44	[39, 52]
Region V	21	[18, 25]	19	[17, 21]	19	[17, 21]
Region VI	12	[10, 18]	13	[10, 18]	13	[10, 18]
Region VII	-	-	42	[40, 45]	42	[40, 45]
Region VIII	-	-	30	[28, 32]	30	[28, 32]
Region IX	-	-	45	[42, 48]	45	[42, 48]

It has been shown that Region II presents an irregular post-fire behaviour which may be due to changes in the ecosystem structure. Since these changes are impossible to assess using this methodology, any conclusions about Region II should be evaluated by field studies or using other vegetation indexes such as EVI.

In Region I, the fit of the model to time-series (i) leads to an underestimation of recovery times, which in case of (ii) and (iii) are 14 months longer. Observation of the complete 11-year time-series for Region I (Fig. 17) indicates that, in fact, vegetation did not recover completely, since *y* values observed in the last years of the time series present a stagnation of lack of greenness values under 90% of the median, the value assumed to correspond to recovery. These low values are almost inexistent over the pre-fire period, with the exception of a few months with values of *y* markedly below 90% of the median, most of them observed during the two droughts of 1998/99 and 2001/02 (Gouveia et al., 2009) and three in 2000. Region I presents some months around winter 2007 with values of *y* above 90% of the median, however there seems to have been a disruption of the regeneration process since a marked decrease is observed during 2007, followed by a stagnation of the lack of greenness. It is impossible to assess the reason for these disruptions of vegetation recovery, which can be either due to natural events or to human intervention. As for Region III, the model fit to time-series (i) led to an overestimation of recovery time of 14 months respecting to the complete time-series and of 16 months respecting to (iii). This is due to the effect of the drought event of 2004/05, and will be analysed further on.

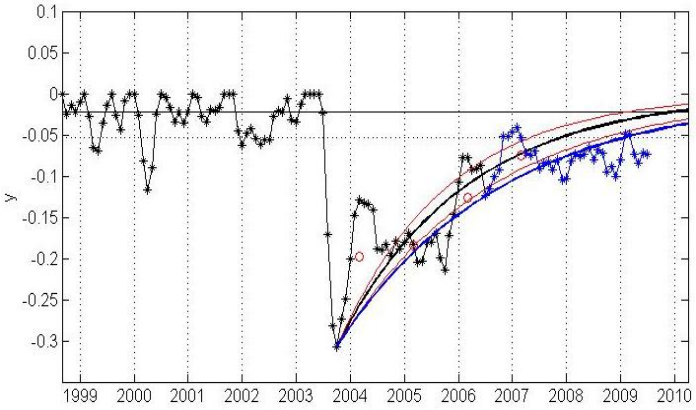

Fig. 17 – As in Fig. 16 but respecting to the burnt scar in Region I.

Use of criterion (iii) does not lead to different results except for Regions II and III. However, in Region III the difference in estimated recovery times is not particularly significant, just two months, and the results of (iii) provide a better adjustment of the model to the observed values than (ii), as revealed by the narrower 95% confidence interval.

It has been shown that the mono-parametric model developed by Gouveia et al. (2010) is able to provide good estimations of vegetation recovery times, even with post-fire time-series of moderate extent. Since the adaptation of the mono-parametric model respecting to criterion (iii) provided better adjustments of the modelled curve to the observed values, it will be used in this work to analyse post-fire vegetation dynamics. It must be stressed that the model provides a satisfactory assessment of vegetation recovery time, as obtained using NDVI, unless the regeneration process is disrupted by any extreme natural event or human intervention. Naturally, in those particular cases, recovery no longer presents post-fire vegetation with analogous behaviour, and must be studied carefully.

3.2.3 Sensitivity to missing data

In the previous section, it was shown that the removal of certain values of the regression analysis led to differences in recovery time estimations. Therefore, the effect of missing data in different periods of the time-series on the model's estimations must be tested, in order to evaluate the model robustness.

The analysis was performed over the burnt area on Region VIII, which had an undisrupted recovery process and where the model provided a very satisfactory adjustment, as shown in Fig. 18. The estimated recovery time for this area was 30 months, with a 95% confidence interval of [28, 32].

Twelve values were removed from the observed lack of greenness time-series since droughts last typically about a year. The values were set to missing data according to the following four cases:

a) Missing values are distributed randomly in the time-series in the period following the fire;

b) Data is missing on the first months after the fire event;

c) Data is missing during the regeneration period;

d) Data is missing for the first months after recovery is achieved.

The time-series of the observed and modelled values of lack of greenness for these four situations are presented in Fig. 19. It is clear that, in all four cases, the modelled curve is only slightly affected by the inexistence of certain values, even if one complete year of the time-series is missing.

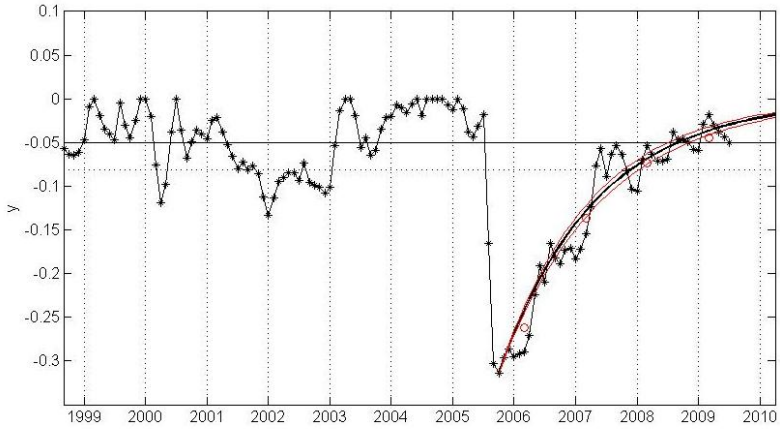

Fig. 18 – As in Fig. 15 but respecting to the burnt scar in Region VIII.

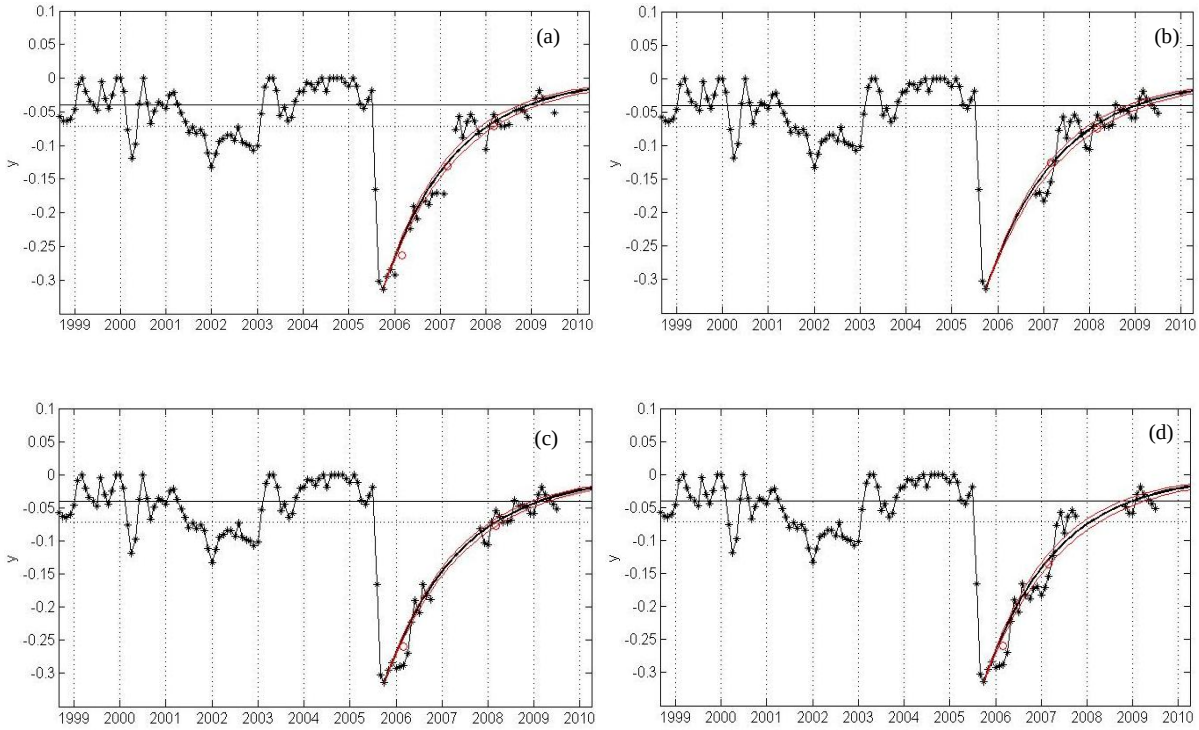

Fig. 19 – As in Fig. 15 but respecting to the burnt scar in Region VIII, tested for the four hypotheses of missing data: a) missing values distributed randomly over the period after the fire event (upper left panel); b) data missing for the year following the month of fire (upper right panel); c) data missing during the recovery period, in the second year following the fire (lower left panel); d) data missing after complete recovery, in the third year after the fire(lower right panel).

Table 2 summarizes the results obtained in the estimation of recovery times and respective 95% confidence intervals for the baseline (no missing data) and for all the four cases of missing data. The highest deviations observed are just 1 month from the standard recovery time (30 months) for cases a) and c), falling within the 95% confidence interval estimated for the basic situation. For the other two cases, no differences respecting to the baseline are observed in estimated recovery times as well as in the 95% confidence intervals. For the evaluation of the effect of random missing files, several tests were performed with different results, however, no significant deviations were observed, since estimated recovery times belong to the 95% confidence interval of the baseline, which is quite narrow. These deviations seem to lead to shorter recovery times when missing vales are sparsely distributed in the time-series (as in case a) in Fig. 19) or, when, missing values are aggregated, to follow the

behaviour of one of the other three cases considered, which, as mentioned before, may not present any difference in the estimation of recovery times.

Table 2 - Vegetation recovery time (t_R) and respective 95% confidence interval ($I_{95}[t_R]$), in months, as estimated by the mono-parametric vegetation recovery model for the burnt scar in Region VIII, for the baseline (no missing data) and for the four cases of missing data as shown in Fig.15, where t_0 is defined as the month use to set parameter *a* of the regression.

Missing data (months)		**t_R (months)**	**$I_{95}[t_R]$ (months)**
-		30	[28, 32]
a)	Random	29	[27, 31]
b)	[t_0+1, t_0+12]	30	[28, 32]
c)	[t_0+13, t_0+24]	31	[29, 32]
d)	[t_0+20, t_0+31]	30	[28, 32]

It is clear that the model is able to provide good estimations of recovery times even when the time-series presents discontinuities. The model also seems to be rather independent of the position of missing data along the time-series. The model seems, therefore, to be quite robust in what concerns missing data on a time-series when the regeneration process is regular. Nevertheless, this conclusion may not be valid for burnt scars which present disturbances in the regeneration process, such as the scar in Region I.

As shown in Fig. 20, vegetation dynamics over the burnt scar in Region I, presents disturbances during post-fire recovery and several years after the fire (as pointed by the red ellipses), which affect the model's estimations. The values corresponding to the months where disturbances are identified were removed in order to evaluate the influence of missing data on those periods in the model's estimations, as resumed in Table 3.

Table 3 – As in Table 2 but respecting to the burnt scar in Region I for the baseline (no missing data) and for the cases of missing data after the first year of recovery and of missing data in the last twelve months of the time series.

Missing data (months)	**t_R (months)**	**$I_{95}[t_R]$ (months)**
None	65	[61,71]
[t_0+13, 132]	21	[16, 30]
[108, 132]	50	[45, 55]

In fact, as pointed earlier in this work, vegetation over Region I seems to have never accomplished recovery in spite of an estimated recovery time of 65 months. In the case when there were just values one year of data after the fire event, the model predicts considerably shorter recovery times (21 months), since disturbances happen only in 2005 and in the last two years of the time series. The first months following the fire are characterised by a rapid increase in *y* values, which is interrupted by the drought of 2004/05, and push the regression curve to higher values. On the contrary, the values corresponding to the last months of the time-series, when stagnation in vegetation activity is registered, seem to push the modelled curve to lower values of *y*.

As shown in Table 3, the lack of information about last months of the time-series leads to an underestimation of recovery times with marked differences. This is to be expected since the model is

based on the premise that the regeneration process is regular. Nevertheless, it is important to acknowledge that external disturbances mislead the model's estimations and, hence, that each analysis must be performed with due care.

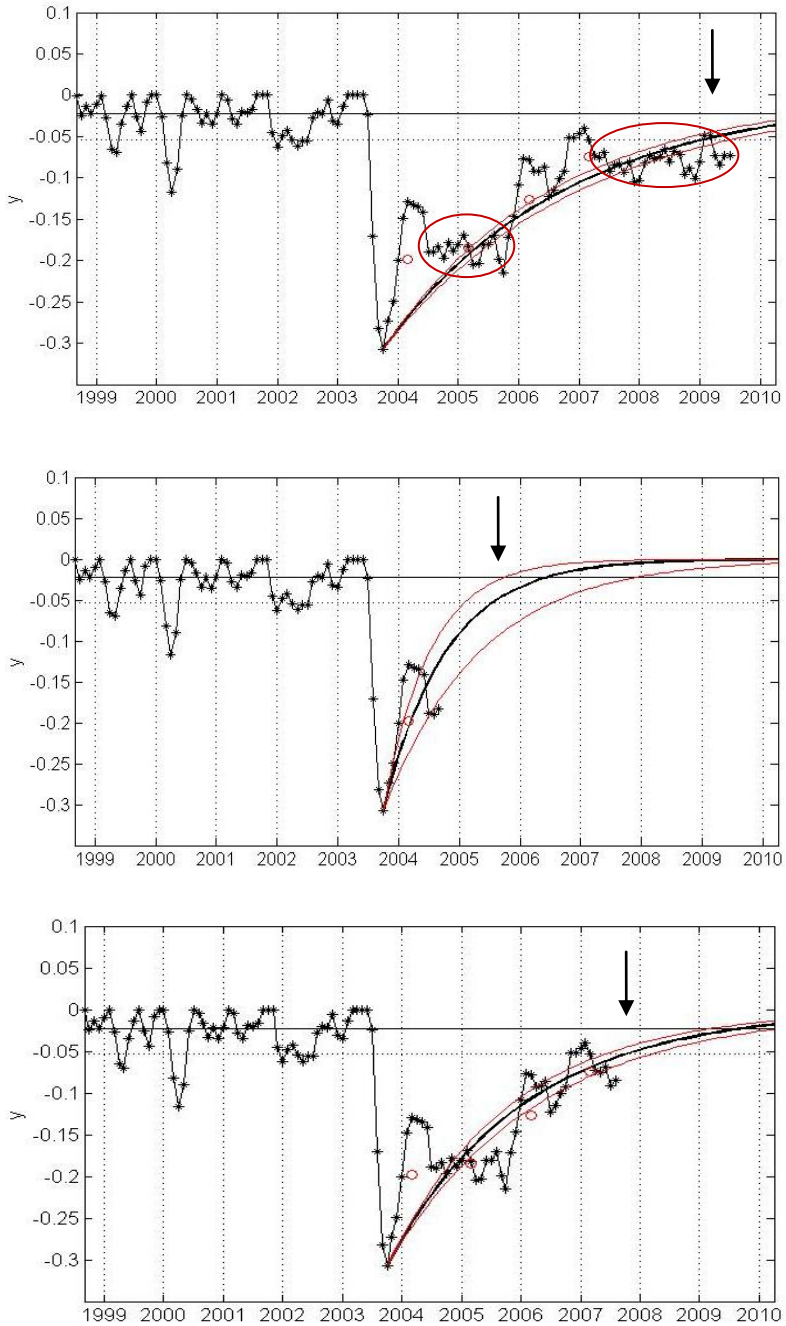

Fig. 20 – As in Fig. 15 but respecting to the burnt scar in Region I, when tested with the three cases of missing data in Table 3.

3.2.4 Sensitivity to drought

Portugal suffered an exceptional drought in 2004/05. According to Gouveia et al. (2009), 65% of the area of Continental Portugal registered monthly anomalies of NDVI below -0.025 for 9 or more months. These exceptional water-stress conditions had a strong impact on vegetation dynamics, and therefore may have affected post-fire vegetation recovery. In fact, over the burnt scars in Regions III and IV, from the 2003 fire season, drought seems to have negatively biased the model, as shown in Fig. 21.

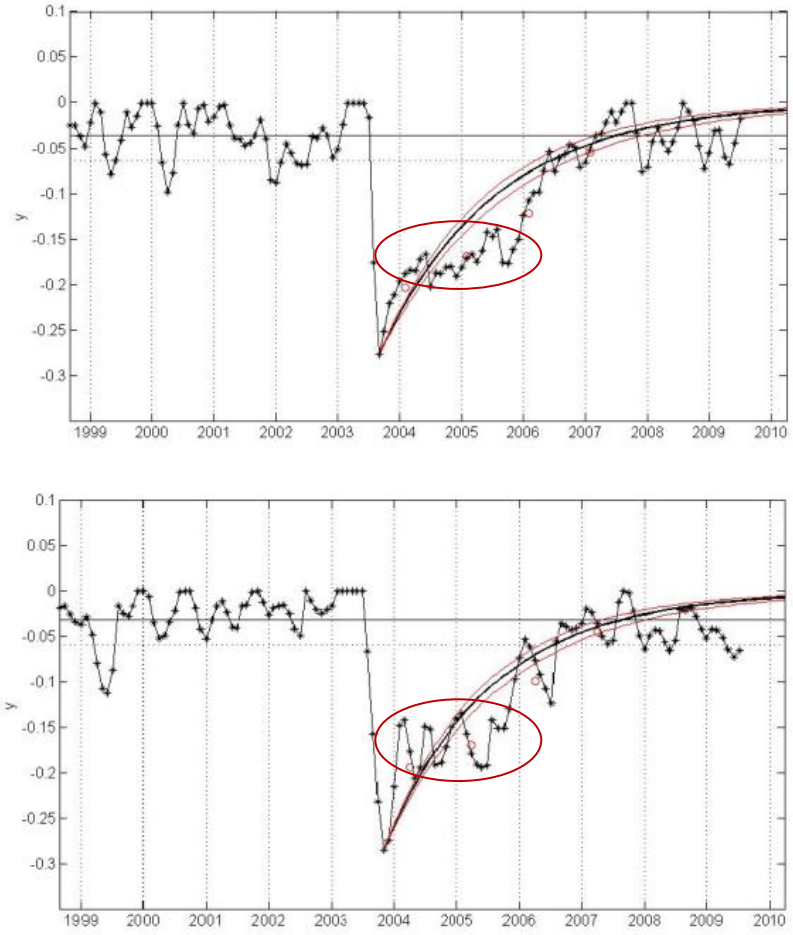

Fig. 21 – As in Fig. 15 but respecting to the burnt scars in Region III (top panel) and Region IV (bottom panel). Red ellipses indicate the effect of the 2005 drought.

In order to understand how drought affected the model's estimations of post-fire vegetation recovery, the values of lack of greenness for the months of drought were set as missing data. Drought was defined as the period of 9 or more months with negative monthly anomalies of the lack of greenness below -0.025, averaged over a non-burnt control area surrounding each fire scar. Monthly anomaly time-series were averaged over the burnt (389 pixels for (a) and 832 pixels for (b)) and non-burnt control areas (865 pixels for (a) and 1800 pixels for (b)). As shown in figures 22 and 23, the drought period corresponds to the months with NDVI anomaly lower than -0.025 in the control area, which were set as missing data in the lack of greenness observed time-series.

Drought lasted for 15 months for Region III and 16 months for Region IV. A previous episode was registered for Region IV in 1999, when another severe drought affected the south of Portugal (Gouveia et al., 2009), however it was not considered in this analysis. It may be observed that the curve for the drought-corrected model (Fig. 22 and 23) fits better the observed *y* values than the uncorrected model (Fig. 21), especially for the first months after the drought period. Excluding the drought data leads to differences both in estimated recovery times and their 95% confidence intervals. Table 3 summarizes

the results obtained by the model before and after excluding drought data. Recovery times estimated by removal of drought months from the time-series are considerably shorter, 6 months for Region III and 8 months for Region V, than recovery times estimated with the complete time-series. This result would be expected since the negative effect of drought is eliminated.

When data corresponding to the months of drought are removed, recovery times are considerably shorter and provide a good estimation of the recovery time if the scar was not affected by drought. The extreme water stress conditions to which vegetation is subject during drought events seem, therefore, to delay the regeneration process, which is to be expected since water availability is determinant to primary productivity and, as shown in Gouveia et al. (2009) this drought was contemporaneous with the period of high photosynthetic activity.

It must be noted that this analysis may not be always required, since the response to drought depends on the ecosystem composition and structure, and also on other environmental factors. For instance, the removal of drought data of the time-series for burnt scar in Region I, which has revealed to be particular sensitive to missing data, leads to a difference of estimated recovery time of just one month (66 months) respecting to the complete time-series (65 months). Setting the values corresponding to the drought period as missing values leads to different results in the areas where vegetation regeneration is considerably affected by water-stress conditions, but seems to have little or no effect in those areas where vegetation recovery is only slightly affected by drought or when the vegetation structure and composition has changed.

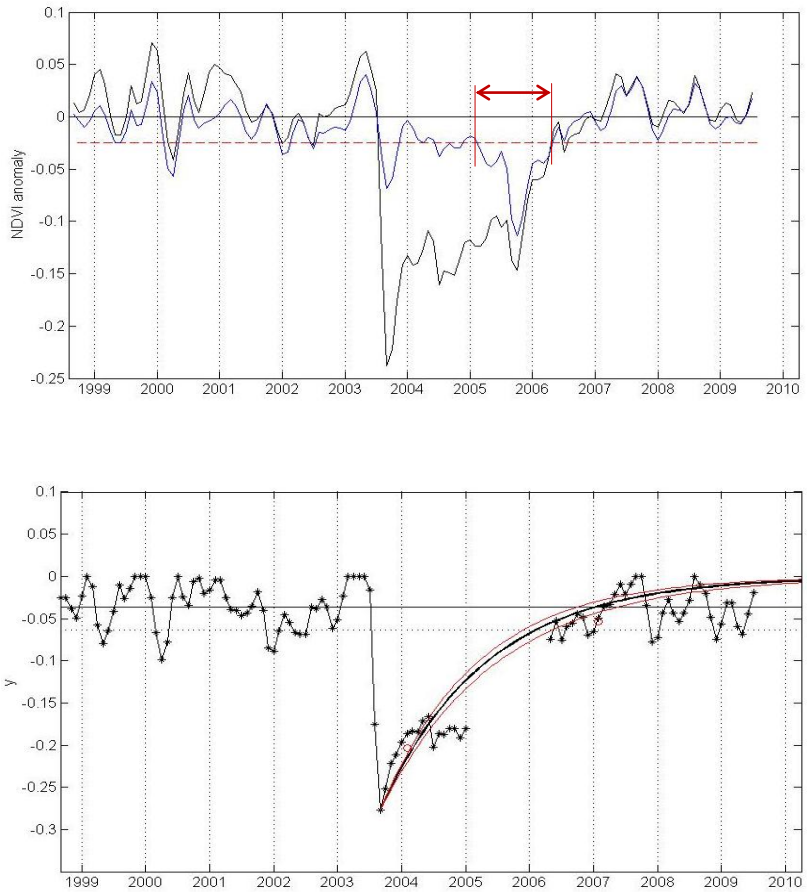

Fig. 22 – Monthly NDVI anomaly time-series (upper panel) averaged over the burnt area in Region III, (black line), and over the corresponding control area (blue line). The dashed red line indicates NDVI anomaly threshold of -0.025. Red vertical lines and horizontal arrow indicate the drought period. Time-series of observed (black line with asterisks) and modelled (black line) NDVI anomaly and time-series of the lack of greenness (lower panel), spatially averaged over the burnt scar, after setting values corresponding to the drought period as no-value data.

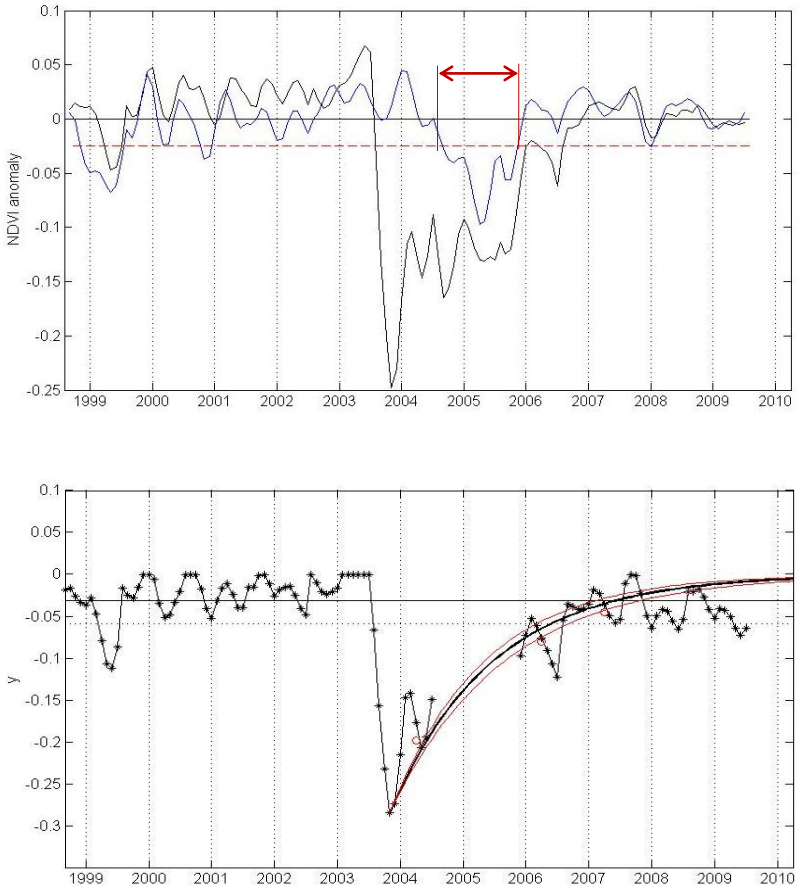

Fig. 23 – As in Fig. 22, but respecting the burnt area IV.

Table 4 – Vegetation recovery time (t_R) and respective 95% confidence interval ($I_{95}[t_R]$), as estimated by the mono-parametric vegetation recovery model for the burnt scars in Regions III and IV. Vegetation recovery time (t_R*) and 95% confidence interval ($I_{95}[t_R]$*),as estimated by the mono-parametric vegetation recovery model after setting the values of observed lack of greenness corresponding to the drought period as missing data.

Burnt area	**t_R (months)**	**$I_{95}[t_R]$ (months)**	**Drought months**	**t_R * (months)**	**$I_{95}[t_R]$ * (months)**
Region III	42	[38, 46]	15	36	[33, 40]
Region IV	44	[39, 52]	16	36	[33, 40]

4. Case-studies

A selection of burnt scars was made with the aim of performing a more exhaustive analysis of vegetation dynamics, particularly to determine spatial patterns and assess the influence of biological and environmental factors on post-fire vegetation recovery. For each burnt scar, the ecosystem's composition was characterized based on the land-cover distribution over the area from the CLC 2000 dataset. Four regions were chosen, covering large scars from fire events which occurred in 2003 (Region III), 2004 (Region V) and 2005 (Regions VII and IX) fire seasons, located in different geographical regions in Continental Portugal and with distinct vegetation composition.

The methodology described in the previous chapter was applied to each burnt area as well as to individual burnt pixels, in order to assess spatial variability of vegetation recovery. The spatial distribution of recovery times was analysed and compared to pre-fire conditions (evaluated by the median of the NDVI over the years preceding the fire occurrence) and to fire damage, in order to assess the influence of these factors on post-fire regeneration. This analysis was based on results from K-means clustering as described in section 3.1. Fire damage was simply estimated by computing the normalized difference of the NDVI values on the months of May of the considered fire season and of the following year. Distribution of recovery times for the most representative land-cover classes was also assessed. The influence of terrain characteristics, such as altitude and slope aspect, on post-fire recovery was also investigated.

4.1 Region III

Region III is located in central Portugal, as shown in Fig.10, and covers a large burnt scar from a fire episode that occurred in the 2003 fire season. The burnt scar has an extension of about 41300 ha (413 pixels) and is mainly occupied by coniferous forest (71%) and transitional woodland-shrub (16%), as shown in Fig.24. According to AFN, coniferous forest in this region is mainly composed by *Pinus Pinaster* species. There are three pixels classified as water bodies, which is due to the existence of a mosaic of land-cover types (as result from the degradation process) that, nevertheless, influences NDVI measurements.

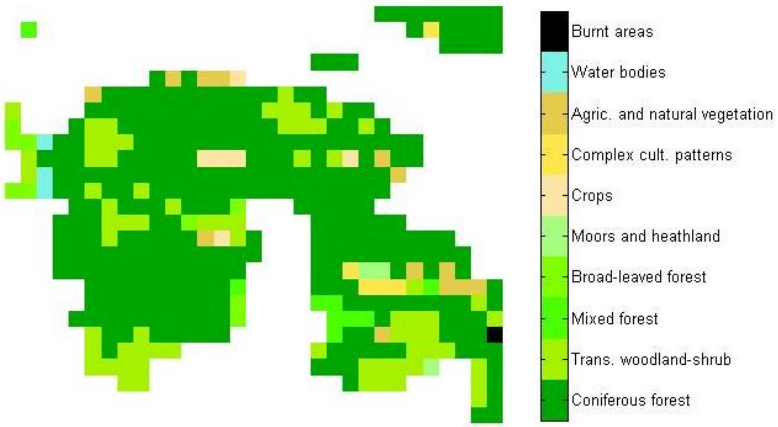

Fig. 24 – Land-cover map over the burnt scar (413 pixels) in Region III, according to CLC 2000 classes shown in the colorbar.

Analysis of vegetation dynamics over the MVC-NDVI time series indicates a marked decrease of NDVI in the month of the fire, clearly visible in the time-series of NDVI and in *y* (Fig. 25) as well as in the NDVI field on the month of May of the following year (Fig. 26). Five years after the fire, in May 2008, the NDVI field shows a photosynthetic activity comparable to the high values registered before the fire. In fact, the average vegetation recovery, defined by the threshold of 90% of the mean

value of the spatially averaged lack of greenness over the pre-fire period, was reached 42 months after the fire event, within a 95% confidence interval of [38, 46] months.

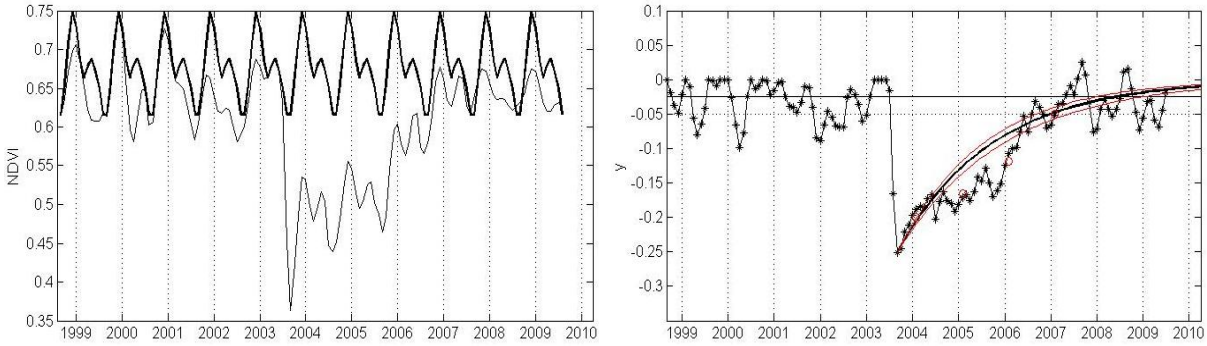

Fig. 25- NDVI (grey line) and GY (black line) time-series (left panel) spatially averaged over the burnt scar in Region III. Time-series of observed (black line with asterisks) and modelled (black curve) lack of greenness, averaged over the burnt area (right panel). Red curves indicate 95% confidence limits of the regressed curve and red circles indicate annual means of *y*.

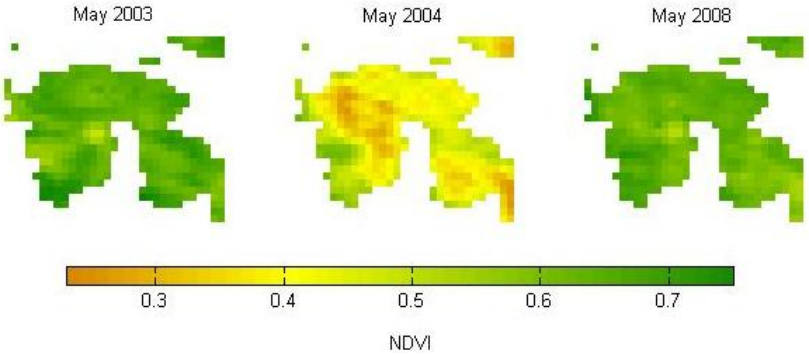

Fig. 26 – Mean NDVI fields over burnt scar in Region III on May of 2003, 2004 and 2008.

This result was affected by the severe drought, as discussed in section 3.2.4. Nevertheless, there are spatial features that present distinct behaviours, such as the large patch in the centre of the scar that seems to have been affected in a higher degree by fire (with very low values of NDVI in May of 2004) or the small area in the southern-east boundary of the scar which is slightly greener in May of 2004 than in the year before, and is one of the areas with higher photosynthetic activity five years after the fire. Therefore, a further study of spatial variability is worth being undertaken.

The variability observed in the NDVI field in May 2004 is analogous to the spatial distribution of estimated recovery times, which tend to aggregate in homogeneous patches, as shown in Fig. 27.

In order to understand the relationships between recovery times, fire damage and pre-fire conditions, K-means clustering was applied to the pairs $\{t_R, NDVI_{2004}\}$ and $\{t_R, NDVI_{MEDIAN}\}$, for the two main land-cover classes (representing more than 87% of the pixels). Although pixels corresponding to other land-cover types would possibly have some effect on the cluster analysis, they were not considered because of their reduced extent It may be noted that $NDVI_{2004}$ refers to the NDVI field in May 2004 whereas $NDVI_{MEDIAN}$ refers to the median value of NDVI during the pre-fire period and provides an estimation of vegetation density before the fire. As shown in Fig. 28 (upper panels), three centroids were identified in both analyses with clearly distinct relationships with the recovery times. These differences may be justified by distinct physical relationships between each variable and the recovery times. However, this assumption must be checked carefully, by studying the spatial distribution of the clusters (lower panels), as well as the dispersion diagrams of their centroids.

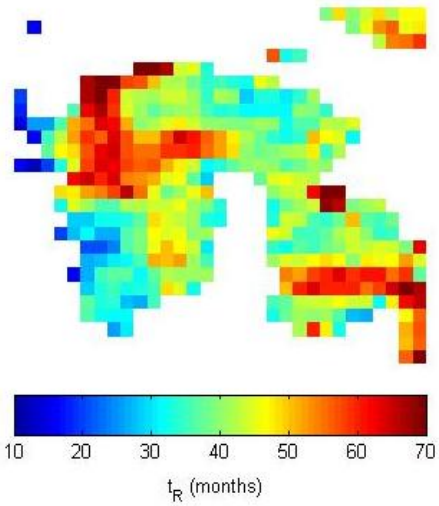

Fig. 27–Spatial distribution of recovery times (in months) as estimated by applying the described methodology to each pixel.

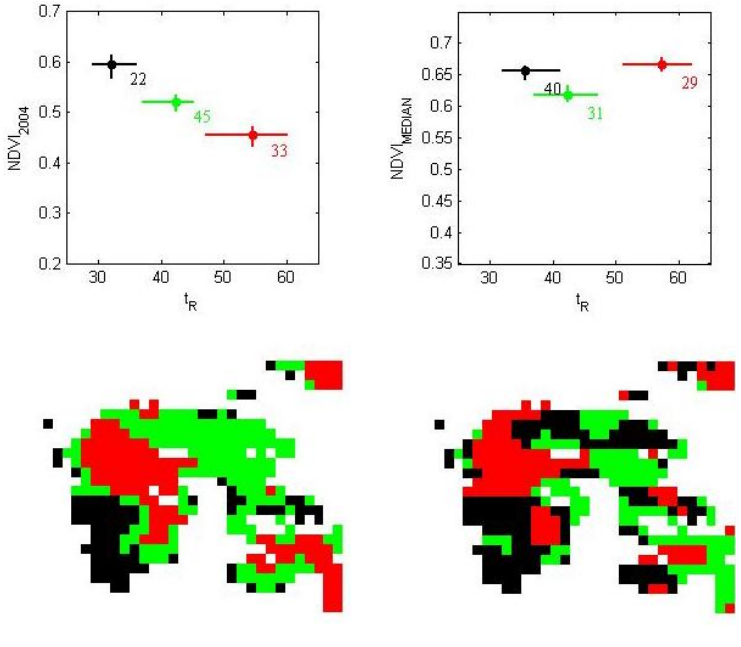

Fig. 28 – Dispersion diagrams (upper panels) and spatial distribution (lower panels) of clusters, identified by distinct colors, as obtained by applying the K-means clustering to the pairs $\{t_R,NDVI_{2004}\}$ (left panels) and $\{t_R, NDVI_{MEDIAN}\}$ (right panels), for Region III. Coordinates of the centroids of each cluster are identified by circles in the dispersion diagrams; horizontal and vertical bars indicate interquartile ranges. Integer numbers near each centroid indicate the fraction of areal cover (%) by each cluster.

The dispersion diagram of the three centroids obtained from the pair $\{t_R,NDVI_{2004}\}$ clearly suggests a near-linear relationship between the two variables, as the recovery time tends to increase with decreasing $NDVI_{2004}$, and shows distinct variability ranges of the three clusters in both variables, since the interquartile ranges do not overlap. Additionally, the spatial distribution of the three clusters is quite similar to the distribution of observed patches in the NDVI difference and recovery time fields. The result is quite distinct in the case of the dispersion diagram of the three centroids obtained from the pair $\{t_R, NDVI_{MEDIAN}\}$, which does not seem to present any monotonic relationship between pre-fire vegetation density and recovery times. Also, the two centroids corresponding respectively to faster (35 months) and to slower (57) recovery times present approximately the same value of pre-fire

vegetation density, which indicates that regeneration over burnt scar III is independent of this parameter.

The vegetation recovery process in this burnt scar seems, therefore, to have been determined mainly by the degree of the destruction caused by the fire event. This relationship would naturally be expected, since the dominant vegetation species is *Pinus Pinaster*, whose regeneration is especially affected by fire severity (which is determinant of the level of fire damage). In fact, both tree survival and post-fire germination of seeds seem to be determined by the exposure to certain temperature thresholds (Pérula et al, 2003; Fernandes and Rigolot, 2007). Therefore, the analysis of the NDVI field in May of the year following the fire event, proves to be adequate for the evaluation of fire intensity/severity.

It is also worth assessing whether this methodology allows the distinction of recovery behaviour for the different vegetation types that compose the ecosystem. A cluster analysis of the recovery time was performed using the K-means method which allowed identifying three centroids with distinct mean recovery times and vegetation composition, as shown in Table 5.

Table 5 – Land-cover distribution over the three centroids as identified by the cluster analysis of the recovery time for Region III.

t_R centroid (months)	Land-cover (CLC2000)	Areal cover (%)
30	Coniferous forest	60
	Transitional woodland-shrub	25
	Other	15
44	Coniferous forest	80
	Transitional woodland-shrub	10
	Other	10
61	Coniferous forest	68
	Transitional woodland-shrub	22
	Other	10

The vegetation distribution over the three centroids is clearly non-uniform and differences between clusters must be analysed in order to evaluate whether they indicate distinct behaviours of the two land-cover classes considered. Coniferous forest predominates in the centroid corresponding to average recovery time (44 months), with an areal coverage of 80%, considerably higher than the fraction of the same vegetation type over the entire region (71%), and transitional woodland-shrub represents just 10% of this cluster. Transitional woodland-shrub covers 16% of the whole burnt scar, however it represents 26% and 24% of the pixels corresponding to lower and higher recovery time, respectively.

Mediterranean dwarf/shrub vegetation is well adapted to fire, being composed by many species of resprouters which recover very rapidly after fire events. On the contrary, coniferous rely on post-fire seed germination to recover after fire, which requires more time. The trend for domination of dwarf/shrub vegetation in the first months following fire events, due to its rapid regeneration process, has been documented (Pérula et al. 2003, Naveh, 1975). These characteristics may justify the differences observed between the centroids with mean recovery time of 30 and 44 months, since coniferous forest clearly dominates the cluster with higher recovery time and transitional woodland-shrub occupies a large fraction of the cluster corresponding to lower recovery times. However, the cluster with highest mean recovery time presents land-cover composition similar to the cluster corresponding to lower recovery time, which indicates the existence of other factors that may influence post-fire recovery.

In fact, although distinct behaviours in post-fire recovery are observed between different vegetation types, the driving factor of post-fire vegetation recovery over Region III seems to be fire damage, as mentioned previously. The existence of different levels of fire damage may also explain the differences observed in recovery time for each land-cover type. The centroid presenting mean

recovery time of 61 months corresponds to pixels highly damaged by fire which take more time to re-establish pre-fire vegetation density. The larger presence of transitional woodland-shrub in this cluster may indicate that this vegetation type was affected more severely by fire, an assumption that is consistent with the great inflamability observed in shrub communities in the Mediterranean (De Luis et al., 2004).

4.2 Region V

Region V, located in southern Portugal as shown in Fig. 10, covers a large fire scar from the 2004 fire season which has an extension of about 38200 ha (382 pixels) and is mainly dominated by broad-leaved forest (77%) and sclerophyllous vegetation (12%), as shown in Fig. 29. Broad-leaved forest is especially composed by *Quercus Suber* species, according to AFN (2010).

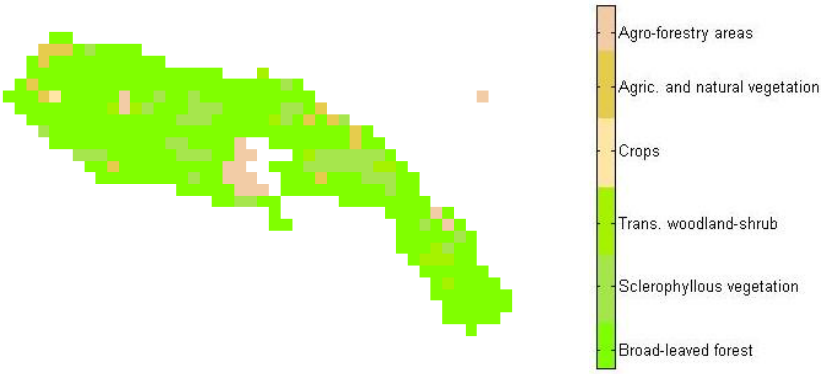

Fig. 29 – Land-cover map over the burnt scar (382 pixels) in Region V, according to CLC 2000 classes shown in the colorbar.

Observation of the vegetative cycle over the 11 years considered and of the *y* time-series, both averaged over the fire scar (Fig. 30), clearly shows that the regeneration process was considerably fast and that the 2005 severe drought, which coincides with the first months of recovery, had little effect on the process. Fast regeneration is confirmed by the estimation of average recovery time of just 13 months, within a 95% confidence interval of [10, 18] months.

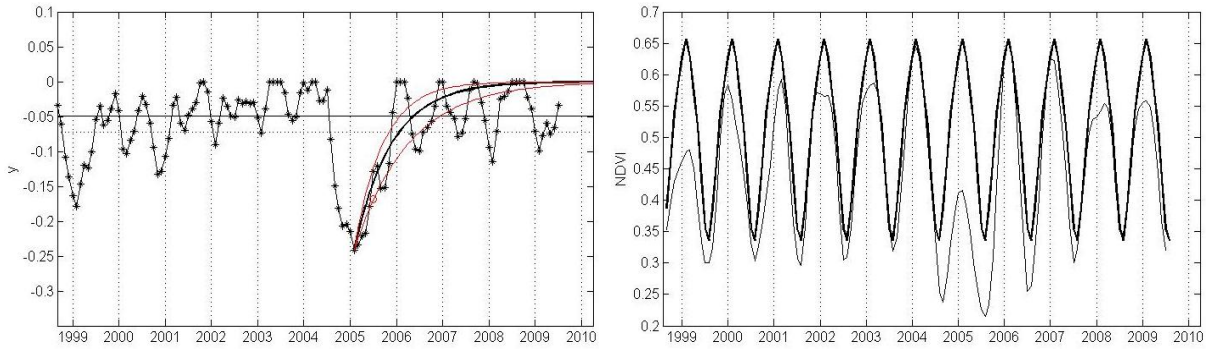

Fig. 30 – As in Fig. 21 but respecting to the fire scar in Region V.

Before the fire event, the region was characterized by high photosynthetic activity throughout the whole area, as shown by the high values of NDVI field in May 2004, in the beginning of the fire season. The field of NDVI one year after the fire occurrence, in May 2005 (Fig. 31), reveals spatial heterogeneity, with one large patch in the western part of the scar presenting marked low values of NDVI, indicating that fire may have been considerably more harmful in this area. In fact, fire damage seems to have been extremely high in this area. However, analysis of spatial distribution of recovery

times (Fig. 32) does not seem to display such clear patches as for fire damage, since high spatial variability is observed.

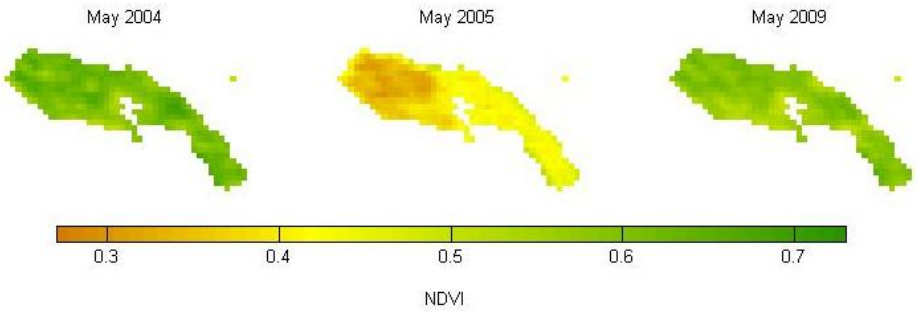

Fig. 31 – As in Fig. 22 but respecting to the fire scar in Region V.

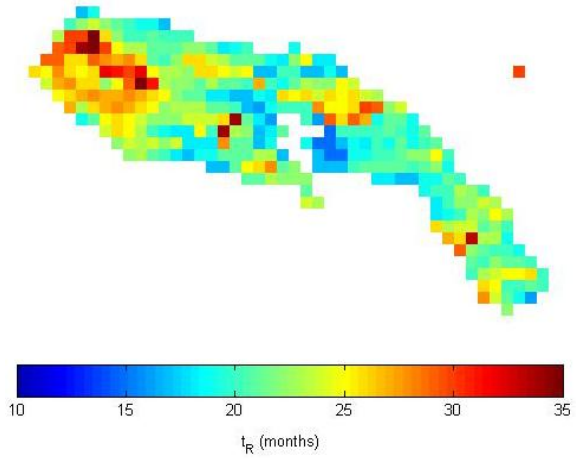

Fig. 32 – As in Fig. 23 but respecting to the fire scar in Region V.

Spatial analysis of the relationship between recovery times and both fire damage and pre-fire conditions provides a better understanding of spatial patterns. A K-means clustering was applied to the pairs $\{t_R, NDVI_{2005}\}$, referring to the NDVI field in May 2005, and $\{t_R, NDVI_{MEDIAN}\}$, referring to the median value of NDVI in May during the pre-fire period, for the two main land-cover classes (broad leaved forest and sclerophyllous vegetation, representing 89% of the area).

Three centroids were identified, as shown in Fig.33, which present dispersion diagrams that are clearly distinct from the analysis of Region III. This indicates the existence of other physical relationships responsible for the recovery time distribution which must be assessed.

In fact, recovery time do not seem to have any particular relationship with the degree of fire damage in this area, as shown by the dispersion diagram of the three centroids obtained from the pair $\{t_R, NDVI_{2005}\}$, which present high variability range in t_R. The centroid with higher values of $NDVI_{2005}$, and therefore less harmed by fire, presents high values of recovery times with superposition of the interquartile range with the interquartile range of the centroid with higher recovery times, indicating that differences between these clusters are especially due to distinct values of NDVI in 2005, more than to differences in recovery times. This assumption is consistent with the analysis of spatial distribution of these three centroids which do not match the spatial distribution of recovery times, indicating that fire damage is not determinant in the regeneration process.

On the other hand, the dispersion diagram of the three centroids as identified from the pair $\{t_R, NDVI_{MEDIAN}\}$ indicates that the recovery time may be related to pre-fire vegetation density, with recovery time increasing with increasing values of $NDVI_{MEDIAN}$. Moreover, the spatial distribution of

the three centroids reveals to be quite consistent with the distribution of the recovery times, since the clusters match the patches observed in the field of t_R. Higher recovery times are observed in those pixels that presented higher vegetation density and photosynthetic activity before the fire occurrence. Therefore, it appears that the recovery time simply corresponds to the period required for vegetation to reach the pre-fire levels of density and complexity, independently of the degree of fire harm.

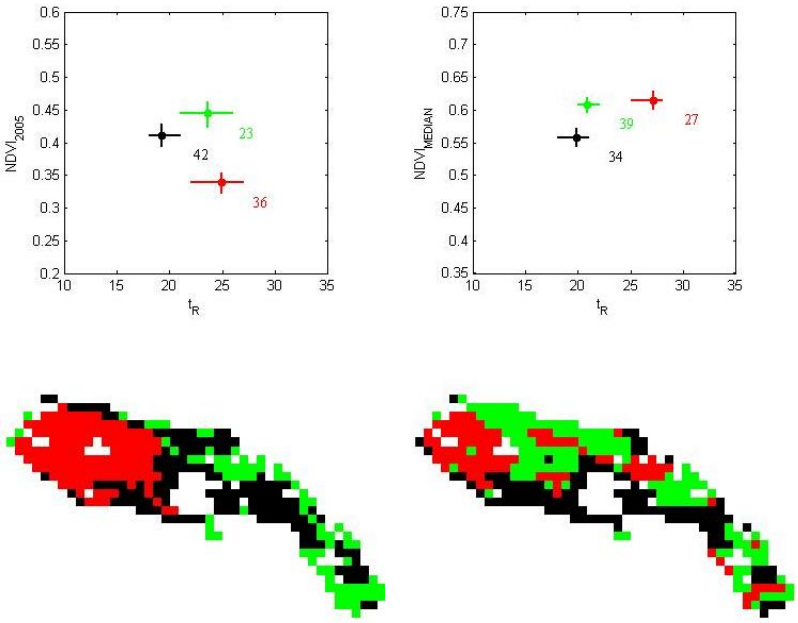

Fig. 33 – As in Fig. 24 but respecting to the fire scar in Region V.

The behaviour of each land-cover class during the regeneration process was also analysed. Cluster analysis of recovery time was performed using the K-means method and three clusters were identified as shown in Table 6.

Table 6 – As in Table 5 but respecting fire scar in Region V.

t_R centroid (months)	Land-cover (CLC2000)	Areal cover (%)
20	Braod-leaved forest	77
	Sclerophyllous vegetation	15
	Other	8
25	Braod-leaved forest	78
	Sclerophyllous vegetation	9
	Other	13
31	Braod-leaved forest	74
	Sclerophyllous vegetation	4
	Other	12

Spatial distribution of the three identified clusters matches spatial distribution of the recovery time field, indicating the existence of areas with distinct behaviour, although the centroids show very similar recovery time, with less than one year of difference between the clusters with shorter and higher recovery time. In spite of some differences in the areal cover of each vegetation type between the clusters – with broad-leaved presenting higher areal coverage in the cluster with mean recovery time of 25 months and sclerophyllous presenting higher areal coverage in the cluster with lower (20 months) mean recovery time – these do not seem to be particularly significant.

The burnt scar is mainly composed by *Quercus Suber*, which is able to survive intense fire events by protecting biomass underneath the thick bark and resprouting from stem buds even if the canopy is entirely burned (Pausas, 1997). Also, most sclerophyll trees and shrubs are obligatory root resprouters, recovering rapidly after fire events (Naveh, 1975).

The two dominant vegetation types present similar post-fire regeneration traits, a characteristic that is consistent with the results obtained by the cluster analysis over this area. No major differences between both vegetation classes in the regeneration process were found, indicating similar post-fire dynamics. However, it is important to stress that the analysis is based on the estimation of soil "greenness" and does account neither for structural changes in the ecosystem's composition nor for individual tree's development. In fact, *Quercus Suber* trees tend to be distributed very sparsely, with shrub or herbaceous vegetation covering the soil underneath. Therefore, pixels may be affected by the rapid growth of herbaceous and shrubs, leading to the observation of high values of NDVI in the first months following the fire independently of tree growth.

4.3 Region VII

Region VII is located in Central Portugal, as indicated in Fig. 10, and covers a burnt scar from a large fire event, occurred in the 2005 fire season. This area has an extension of about 25700 ha (257 pixels) and is mainly occupied by transitional woodland-shrub (45%) and coniferous forest (35%), as shown in Fig. 34. According to AFN, coniferous forest in this region is composed essentially by *Pinus Pinaster* species. As in Region III, three pixels were classified as water bodies, due to the existence of a small fraction of vegetation in those pixels that, nevertheless, influences NDVI measurements.

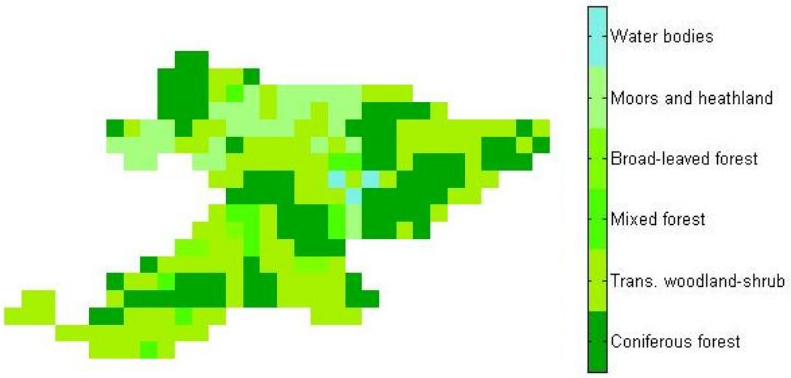

Fig. 34 – Land-cover map over the burnt scar (257 pixels) in Region VII, according to CLC 2000 classes shown in the colorbar.

Observation of the vegetative cycle, represented by monthly values of NDVI averaged over the burnt scar, as well as the lack of greenness indicate an irregular regeneration process, marked by a fast growth in the first year, followed by a long period of near-stagnation (Fig. 35). Although the application of the methodology allowed an estimation of a recovery time of 42 months ($I_{95}[t_R]$ = [40, 45]), recovery does not seem to have been actually achieved, since most *y* monthly values during post-fire period stay below the recovery threshold, as previously discussed in section 3.2.2. Moreover, observation of the NDVI fields (Fig. 36) in May from the year of the fire occurrence (2005), one year after (2006) and four years following the fire event (2009), shows the existence of one large patch, located in the north-eastern region, with low NDVI values in 2009 which seems to have been particularly affected by fire, as observed in the NDVI field in May 2005, and maintains low values of NDVI in May 2009, suggesting incomplete recovery. The spatial distribution of NDVI values in May 2006 (Fig. 36) reveals high variability, as a large homogenous patch with high values of NDVI difference is identified in the north-eastern area, indicating a high level of fire damage, whereas pixels located in the boundary seem to have been slightly damaged by fire, or not affected at all. The high

values of NDVI observed in those pixels may also be due to contamination from unburned pixels in the neighbourhood.

Similar patterns are observed in the spatial distribution of recovery times (Fig. 37), with many pixels located in the north-east presenting recovery times above 50 months and some pixels in the boundary displaying recovery times below 15 months. Some of these pixels located in the boundary present very low values of estimated recovery times and it is difficult to assess whether they were actually burnt or have been contaminated by pixels in the neighbourhood.

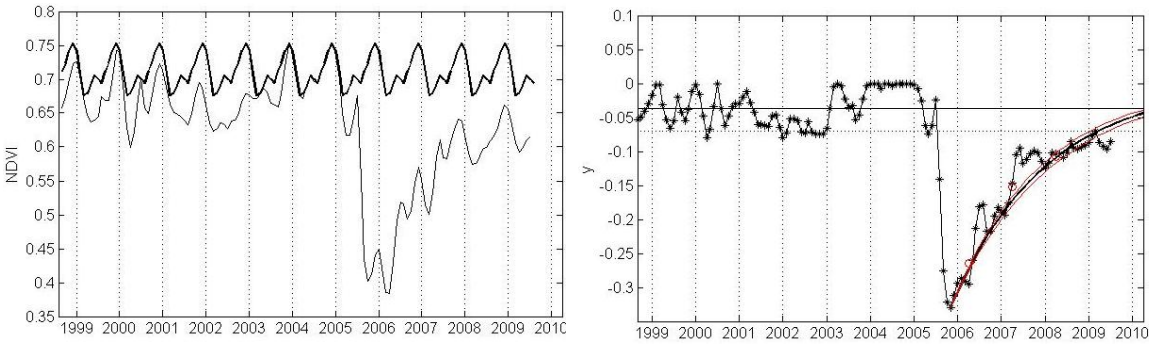

Fig. 35 – As in Fig. 21 but respecting to the fire scar in Region VII.

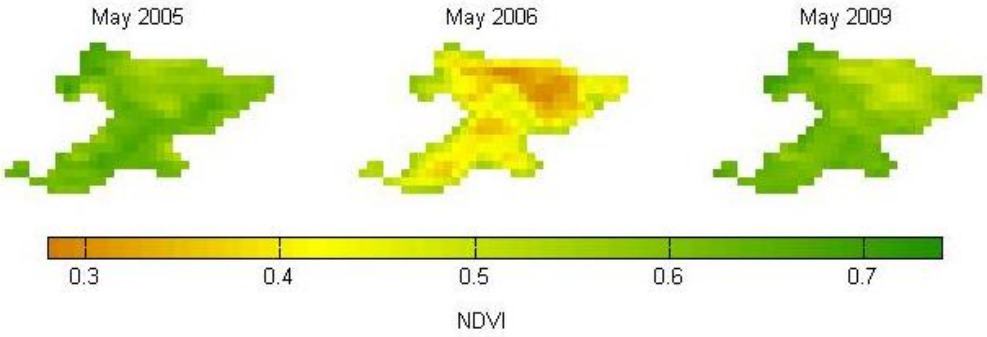

Fig. 36– As in Fig. 22, but respecting to the fire scar in Region VII.

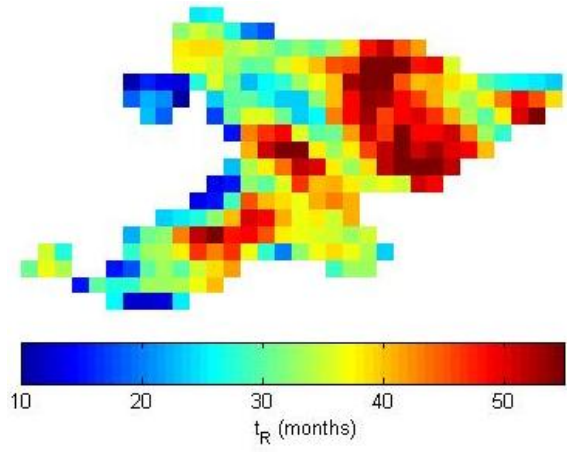

Fig. 37 – As in Fig. 23, but respecting to the fire scar in Region VII.

Further conclusions may be derived from the K-means spatial clustering, when applied to the pairs $\{t_R, NDVI_{2006}\}$ and $\{t_R, NDVI_{MEDIAN}\}$for the two main land-cover classes, in order to understand relationships between recovery times, fire damage and pre-fire vegetation activity, respectively.

The dispersion diagram (Fig. 38, top left panel) of the three centroids as obtained with the pair $\{t_R, NDVI_{2006}\}$ clearly suggests an almost linear relationship between the two variables, with recovery times increasing with decreasing $NDVI_{2006,}$ similarly to results in Region III. The two centroids corresponding to pixels with higher recovery times present relatively small variability in both variables, whereas the other centroid presents larger variability in $t_{R,}$ than in $NDVI_{2006}$ as indicated by the extension of the interquartile ranges. This difference may be due to an hypothetical contamination of the pixels located in the boundary, since the spatial distribution of the latter centroid corresponds to the location of the pixels mentioned before. However, it is clear that fire damage plays a determinant role in post-fire vegetation recovery, since the spatial distribution of the three centroids matches the homogenous patches identified both in the field of NDVI difference and of t_R. It is worth observing that the spatial distribution of the three centroids resembles the distribution of the main vegetation types, as the pixels associated with higher fire damage correspond essentially to pixels of coniferous forests (Fig. 38, bottom left panel).

As for the three centroids obtained with the pair $\{t_R, NDVI_{MEDIAN}\}$, variability in recovery times is considerably higher than in median NDVI values and spatial distribution of the centroids (Fig. 34, right panels) does not seem to match the spatial features observed in NDVI difference and recovery time fields, suggesting that differences between the three centroids are mainly due to the existence of areas with distinct vegetation density before the fire event.

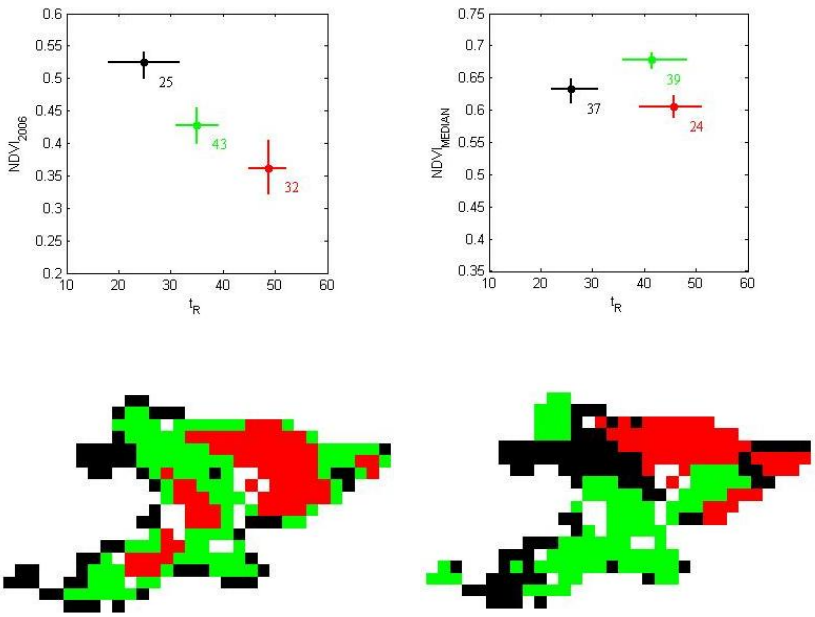

Fig. 38 – As in Fig. 24, but respecting to the fire scar in Region VII

Vegetation recovery seems to be determined, in this region, by the degree of fire damage in vegetation cover, as in the case of Region I. Since *Pinus Pinaster* is one of the main vegetation species in Region III, it would be natural expecting that fire intensity (assessed by the level of fire damage) might affect the regeneration process to some extension. It is interesting to observe that despite the fact that coniferous forest occupies just about one third of the area, the regeneration process over the whole area seems to have a monotonic relationship with fire damage. However, this does not mean that both vegetation types have the same behaviour.

Cluster analysis of the recovery time allowed the identification of three clusters with clearly distinct mean recovery time and land-cover composition, as shown in Table 7. Coniferous forest, which occupies 35% of the area, represents just about 23% of the two clusters corresponding to lower

recovery times, whereas for the cluster corresponding to pixels with slow recovery (50 months) it represents 63%. On the contrary, transitional woodland-shrub occupies the majority (50% and 55% of areal cover) of the two centroids associated with low recovery time (20 and 35 months), whereas for the centroid corresponding to a recovery time of 50 months this land-cover type just represents 24%.

The differences between the three centroids clearly suggest distinct regeneration processes for the two land-cover types considered, as found in Region III but considerably more pronounced. Recovery time distribution over the three centroids is also similar to Region III, although the latter tends to present longer recovery times. Actually, vegetation in pixels corresponding to longer recovery times may have not recovered completely, as observed for the vegetation dynamics averaged over the burnt scar.

Table 7 – As in Table 5, but respecting to Region VII.

t_R centroid (months)	Land-cover (CLC2000)	Areal cover (%)
20	Coniferous forest	23
	Transitional woodland-shrub	50
	Other	27
35	Coniferous forest	23
	Transitional woodland-shrub	55
	Other	22
50	Coniferous forest	63
	Transitional woodland-shrub	24
	Other	13

As referred previously, transitional woodland-shrub tends to recover faster than coniferous forest, which indicates specific recovery traits for each vegetation type and is coherent with the trend to domination of the ecosystem by dwarf/shrub layer in the first years following fire events (Naveh, 1975; Pérula et al. 2003; Cerdà and Doerr, 2005).

4.4 Region IX

Region IX, located in central Northern Portugal as indicated in Fig. 10, covers a burnt scar from the 2005 fire season, with about 10500 ha (105 pixels) of extension and is mainly occupied by coniferous forest (45%) and transitional woodland-shrub (37%), as shown in Fig. 39. According to AFN, coniferous forest is mainly composed by *Pinus Pinaster* species.

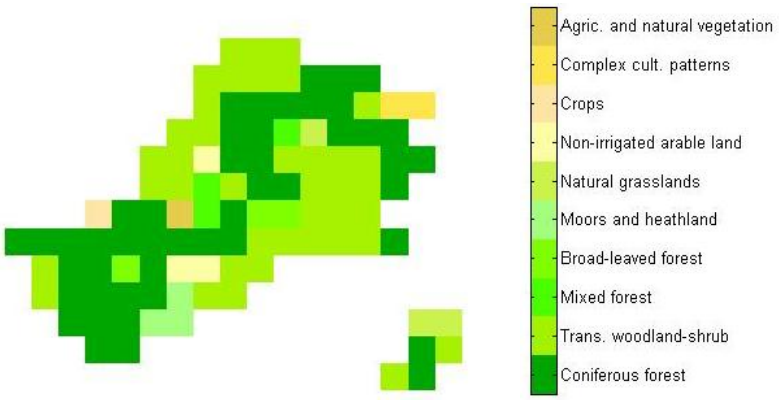

Fig. 39 – Land-cover map over the burnt scar (105 pixels) in Region IX, according to CLC 2000 classes shown in the colorbar.

Vegetation dynamics in this scar, as estimated by the spatially averaged monthly values of NDVI and of the lack of greenness (Fig. 40), presents an irregular behaviour throughout the 11-year time-series and seems to have been disturbed several times, particularly by the 2002 drought which mainly affected North-eastern Portugal and, in lower degree, by the 2005 exceptional drought (Gouveia et al., 2009), indicated by the vertical arrows. As observed in the NDVI field in May 2005 and in *y* time-series (vertical arrow), vegetation was under vegetative stress right before the fire. The regeneration process also presents an irregular behaviour which seems to delay recovery, as defined by the threshold of 90% of the mean value of the lack of greenness over the pre-fire period, estimated to be reached in 45 months ($I_{95}[t_R]$ = [42, 48]). By observing the NDVI fields in May 2005 and May 2009 (Fig. 41), it is possible to identify one region in the southern part of the scar where vegetation seems to be completely reestablished, with higher values of NDVI in 2009 than in 2005, whereas in the eastern area NDVI values in 2009 remain lower that in 2005.

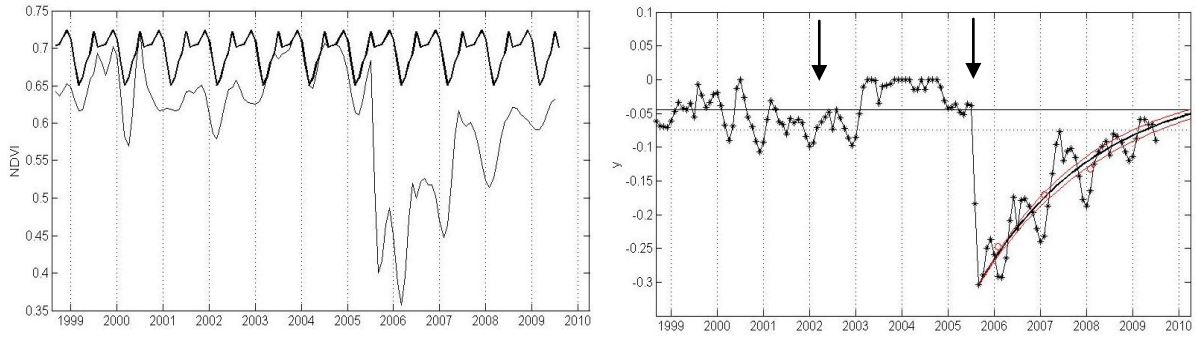

Fig. 40 – As in Fig. 21 but respecting to the fire scar in Region IX.

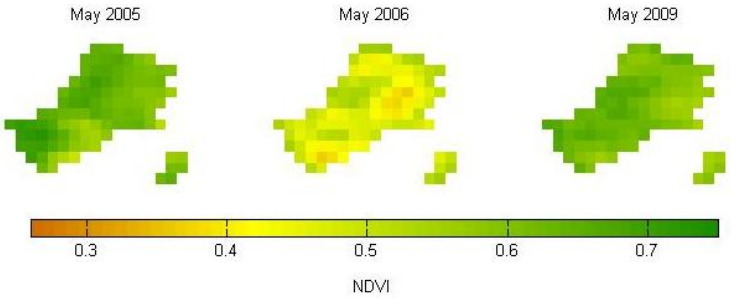

Fig. 41 – As in Fig. 22 but respecting to the fire scar in Region IX.

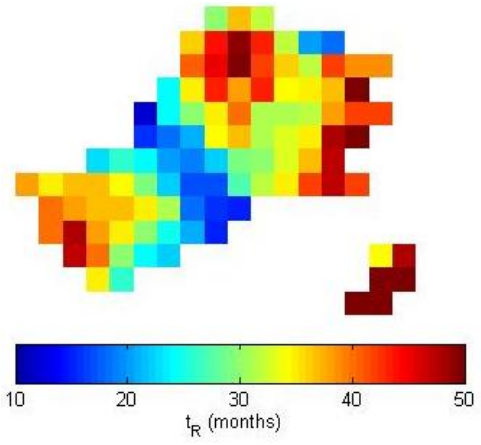

Fig. 42 – As in Fig. 23 but respecting to the fire scar in Region IX.

The majority of the pixels present recovery times lower than 40 months, as shown in Fig. 42 (right panel), well below the estimated recovery time over the scar of 45 months. In fact, the model seems to be affected by some pixels which present very high recovery times, some of them above 60 months.

Spatial cluster analysis, based on the K-means method, was applied to the pairs $\{t_R, NDVI2006\}$ and $\{t_R, NDVI_{MEDIAN}\}$for the two main land-cover classes (Fig. 43), in order to identify possible relationships between recovery times, fire damage and vegetation density, respectively. The dispersion diagram of the three centroids obtained for the pair $\{t_R, NDVI2006\}$ does not seem to suggest any kind of relationship between the two variables. The cluster corresponding to the pixels less harmed by fire presents higher recovery times and a very wide interquartile range which overlaps the interquartile range of the cluster corresponding to pixels with high fire damage. Additionally, the spatial distribution of the three centroids matches the spatial distribution of NDVI difference but does not seem to fit adequately the spatial distribution of recovery times. No clear relationship is also observed in the dispersion diagram of the three centroids obtained for the pair $\{t_R, NDVI_{MEDIAN}\}$, as two of the centroids present almost the same $NDVI_{MEDIAN}$ values but distinct ranges on t_R and pronounced variability. Moreover, the spatial distribution of the three centroids does not seem to match, either, the spatial distribution of recovery times.

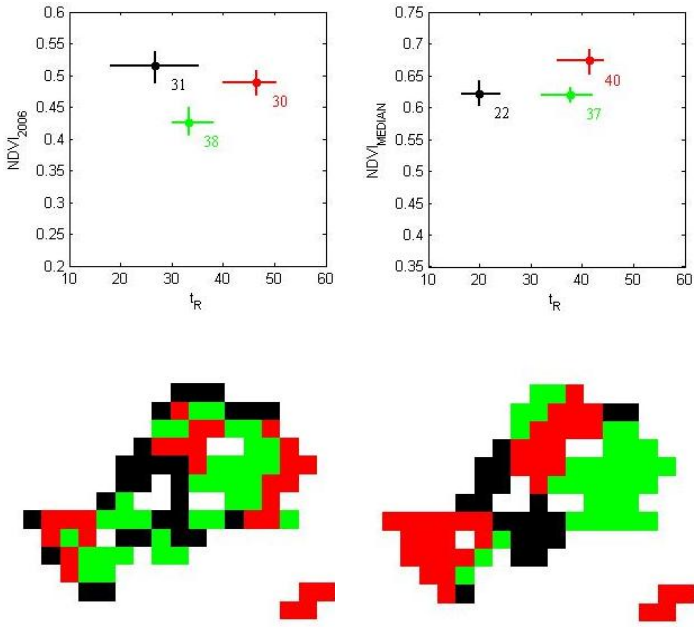

Fig. 43 – As in Fig. 24 but respecting to the fire scar in Region IX.

Since coniferous forest, essentially *Pinus Pinaster*, is the main land-cover in this scar, covering about 45% of the area, one might expect that recovery would be driven by physical relationships similar to those of Region III and VII. However, regeneration does seem to have been determined neither by fire damage, nor by pre-fire vegetation activity, thus a further inspection on the behaviour of the two main land-cover types is required.

A K-means cluster analysis of recovery time was performed, allowing the identification of three centroids with distinct behaviours, as shown in Table 8. As in Region III and VII, coniferous forest tends to dominate the centroid corresponding to longer recovery times (63% of the area) and to present lower areal coverage (35%) over the centroid corresponding to shorter recovery times. Transitional woodland-shrub presents the same distribution over the cluster corresponding to longer recovery times as over the entire area (37%). In the cluster corresponding to shorter recovery times, the fraction of areal cover is lower (32%). It is worth noting the fact that 33% of the area corresponding to the cluster with shorter recovery times is occupied by other land-cover types. It is also worth pointing the fact that none of the pixels from the cluster respecting to longer recovery times is occupied by other vegetation types.

As observed previously, coniferous forest tend to recover slower than other vegetation types present in Region IV, which is mainly due to specific post-fire recovery traits of *Pinus Pinaster* species. Transitional woodland-shrub seems to recover slower than in Region VII, however its almost uniform distribution over the three clusters may indicate diverse behaviours, possibly due to the existence of several species with distinct post-fire recovery characteristics or other factors driving the regeneration process. Other land-cover types in this burnt scar are composed by different sorts of agricultural regimes, the non-uniform distribution observed indicates simply that land was re-cultivated in the first years after the fire.

Table 8 – As in Table 5, but respecting to Region IX.

t_R centroid (months)	Land-cover (CLC2000)	Areal cover (%)
22	Coniferous forest	35
	Transitional woodland-shrub	32
	Other	33
38	Coniferous forest	48
	Transitional woodland-shrub	40
	Other	12
59	Coniferous forest	63
	Transitional woodland-shrub	37
	Other	0

Despite the fact that some differences between vegetation types are observed, it is important to stress that vegetation distribution presents a marked distinction between the three clusters for coniferous, whereas transitional woodland-shrub presents a more uniform distribution over the three clusters. Some pixels present recovery times longer than 70 months but do not seem to have any particular characteristic that could justify their behaviour, since they correspond to several land-cover classes, they have been damaged in different degrees by fire and they are sparsely distributed in the area.

This result may indicate the existence of other physical factors driving the regeneration process, not considered in this analysis, or of an external disturbance of the vegetative cycle during recovery or after recovery is established, as discussed in section 3.2.3. In order to understand recovery dynamics in this scar, it would be necessary to perform a more exhaustive analysis, considering external factors which may influence recovery, such as altitude and slope, and, probably, run field studies which might validate results.

It is worth pointing the existence of patterns in vegetation recovery over Regions III, VII and IX, all composed by coniferous forest and transitional woodland-shrub, as they present close recovery times for the centroids identified. These three areas present one centroid with recovery times of about two years (30, 20 and 22 months, respectively), another centroid with about three years (44, 35 and 38 months) and a last one with a recovery time above four years (61, 50 and 59 months) following the fire event. This indicates the existence of distinct phases in the overall regeneration process, which are related to the specific traits of vegetation. However, the centroid with higher mean recovery time of Region IX differs by 9 months from the centroid in Region VII, and is closer to the value obtained in Region III. The systematically higher values of recovery time for the centroids obtained in Region III may be due to the effect of the 2005 drought event. As for Region IX, the high mean recovery time value for the third centroid respects to those pixels that present recovery times above 70 months, although the reason for such slow recovery cannot be determined.

4.5 Slope dependence

As previously discussed, fire regimes and plant traits determine to a great extent post-fire vegetation recovery. Nevertheless, there are other factors which affect directly or indirectly the regeneration process, such as slope, altitude and composition or climatic conditions (Pausas and Vallejo, 1999). Water availability plays a determinant role in primary productivity and, thus, in post-fire vegetation recovery dynamics. Moisture conditions, more favourable in North facing slopes (less exposed to sun radiation and, therefore, smaller water loss by evapotranspiration) and water retention capacity (higher in flat areas or terraced slopes) provide more favourable conditions for vegetation recovery (Tsitsoni, 1997; Pausas et al., 2004; Fox et al., 2008).

The assessment of terrain influence on post-fire vegetation recovery was based on data from the GLOBE project 1 km resolution DEM as mentioned in chapter 2.4. Slope aspect was evaluated by simply computing the gradient of elevation in N-S and W-E directions. Since differences in vegetation activity between West and East facing slopes are expected to be less marked than between North and South facing slopes, the former were not considered in the present work. The analysis of the relationship between recovery time and slope aspect in the N-S direction was performed over the four regions studied previously in this chapter. Due to the coarse resolution of both NDVI and DEM data (1 km), high variability is expected, since surface roughness at a smaller scale, which has greater influence on vegetation dynamics, is ignored. Information about the distribution of slope over the pixels for each burnt scar is summarized in Table 9, where slope is given in percentage (%).

Table 9 – Statistical distribution (median, lower and upper quartiles) of the computed slope, given in percentage (%), over each burnt scar, for the North and South facing hillsides.

		Region III	**Region V**	**Region VII**	**Region IX**
North	**Median**	2,5	1,5	4,9	10,4
	25%	1,3	0,8	2,0	5,2
	75%	4,1	2,6	9,9	14,0
South	**Median**	2,6	2,5	5,6	7,2
	25%	1,3	1,0	2,7	3,2
	75%	4,3	4,3	8,8	10,4

It is also necessary to take into account that distinct species respond differently to environmental factors. In order to reduce variability due to vegetation characteristics, only forests were considered in the study of each area, which corresponds to coniferous forests in Regions III, VII and IX (mainly *Pinus Pinaster*) and to broad-leaved forests (*Quercus Suber*) in Region V. The distribution of recovery times in each slope was estimated and is shown in Fig. 44.

Distribution of recovery time over Region III does not seem to indicate any especial effect of slope aspect on vegetation recovery, since no major differences are found, neither in the median value of t_R (40 and 38 months for the North and South facing aspects, respectively), nor in the extent of interquartile ranges, which are very similar. In fact, slope over this region is not especially significant, presenting median values of 2.5% and 2.6% on the North and South facing aspects, respectively, and very narrow interquartile ranges. Moisture conditions on both hillsides must be almost identical and, therefore, coniferous trees in the North and South facing aspects follow a similar behaviour. Region I is located at low altitude, between 113 m and 577 m above sea level, thus a faster recovery would be expected. The long recovery times registered, as well as the high variability, may be related to the severe drought which affected this area in 2004/05 and disrupted the regeneration process.

Vegetation of the burnt scar in Region V presents a very quick recovery with a median value of 21 months for both hillsides and considerably low variability. Also, distribution of recovery times is identical on both aspects, indicating that slope is not determinant in the post-fire regeneration process. This region does not present a particularly prominent slope, with very low median values and small variability, indicating similar moisture conditions over both hillsides, and, in addition, *Quercus Suber*

is particularly resistant to water stress conditions. Thus, it is natural that slope aspect over this area does not reveal to be determinant to the regeneration process. Besides, Region V is located at low altitude, between 187m and 554m above sea level, which favours the rapid recovery observed.

On the contrary, both Region VII and IX seem to present distinct vegetation recovery patterns on North and South facing slopes, which are sharper than in other regions. Pixels located in northern aspects tend to recover faster, as indicated by the median values of recovery time of 38.5 and 35 months, respectively, while southern aspects present median values of 49 and 38 months. It is worth stressing the marked contrast in recovery time for pixels located on each hillside of Region VII, with almost one year of difference between the median values and more than six months of difference between the 25% quartiles. Moisture conditions play, thus, an important role in post-fire coniferous recovery in these two scars. This is particularly important for Region IX, where none of the factors studied previously in chapter 4.4 appeared to be driving the regeneration process, and stresses the importance of environmental factors on post-fire vegetation recovery analyses.

In spite of presenting identical relationships between recovery time and slope, the two regions show some differences in recovery time distribution. Vegetation in Region VII tends to recover slower and presents higher variability than in Region IV, as pointed by the interquartile ranges in Fig. 39. This may be partially explained by differences in the altitude at which the burnt scars are located, since Region VII is located between 333m and 1089m above sea level, whereas Region IX is situated between 262m and 932m above sea level.

Results for Regions VII and IX are consistent with other studies of terrain influence on post-fire vegetation recovery for Mediterranean forests which indicate that vegetation recovers more rapidly on North faced slopes and at low or moderate altitudes (Tsitsoni, 1997; Pausas and Vallejo, 1999; Pausas et al., 2004; Wittenberg et al., 2007).

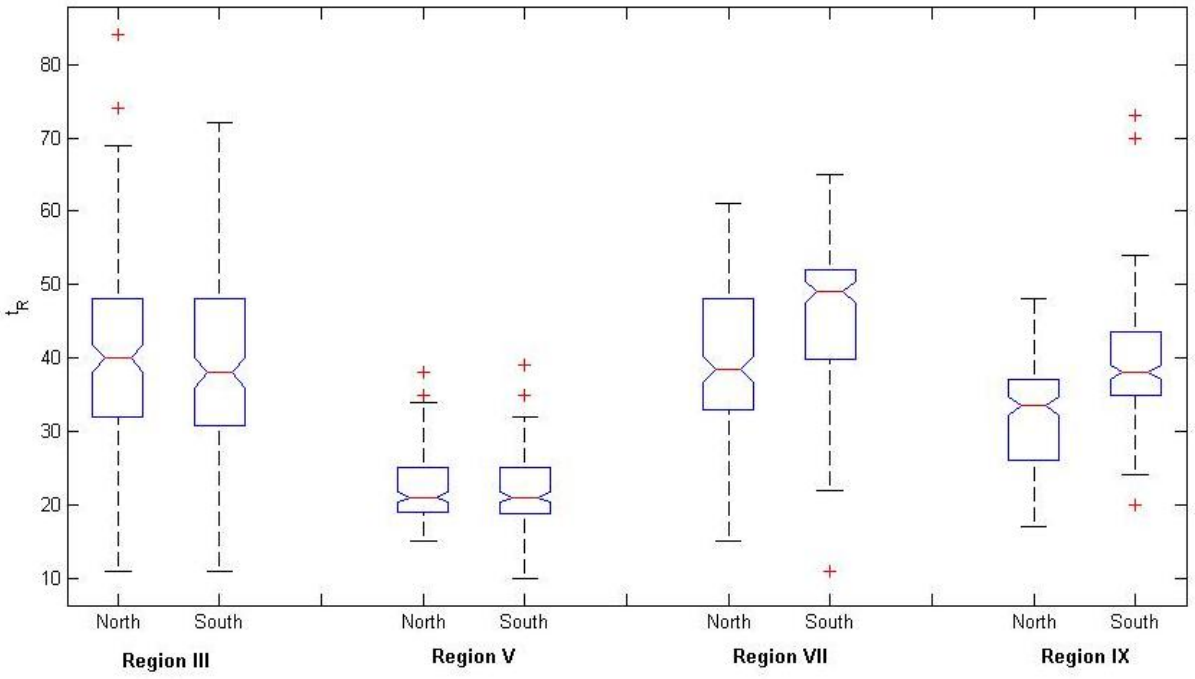

Fig. 44 – Recovery time distribution over each slope aspect (North and South) for Regions III, V, VII and IX. Red lines indicate median values; blue boxes indicate the 25% and 75% interquartile ranges and black whiskers encompass the 1.5% and 98.5% interquartile ranges. Red crosses represent outliers.

5. Conclusions and final remarks

Fires have shaped Mediterranean landscape for many centuries, becoming an integral part of these ecosystems (Naveh, 1975). However, in recent decades, land-use changes and climatic warming have led to a marked increase in the number of fire events, as well as in the extension of surface burnt. Fires became a serious problem, increasing erosion and soil degradation (Pausas and Vallejo, 1999). Portugal is the European Mediterranean country with the highest number of fire events since 1980 and with more burnt area over the last decade (JRC-EC, 2009). The years of 2003 and 2005 were particularly relevant, with the highest number of fire occurrences (2005) and the two maximal values of burnt area since 1980, 425000 ha and 338000 ha, for 2003 and 2005 respectively (DGRF, 2008). These extreme fire seasons further coincide with the heat wave that stroke Europe in 2003 (Pereira et al., 2005) and with the severe drought of 2004/2005 which lasted for more than 9 months in more than one third of the country (Gouveia et al., 2009). As in the Mediterranean ecosystems, fires have in Portugal, ,complex effects on vegetation dynamics, namely on recovery, due to the distinct response of vegetation to diverse fire regimes and, also, due to other factors such as geomorphology and climate. An exhaustive analysis of post-fire vegetation recovery and of its driving factors is crucial to the establishment of adequate land-management practices.

The main goal of the present work was to evaluate the sensitivity of the mono-parametric model developed by Gouveia et al. (2010) to the time-series length and to missing data, as well as to study vegetation recovery following some of the larger wildfires that occurred in Portugal over the last decade, namely in 2003, 2004 and 2005, through the application of the model to remote sensing data. More particularly, the objective was to analyse post-fire vegetation dynamics, estimate recovery times and assess the influence of driving factors, such as fire characteristics, plant traits and environmental factors. An eleven-year analysis of vegetation activity was used, based on monthly composites of Normalized Difference Vegetation Index (NDVI) from the VEGETATION dataset. The methodology relied on the procedure used by Gouveia et al. (2010), which relies on results from (i) spatial cluster analysis to identify fire scars and evaluate relationships between driving factors and recovery time; and from (ii) a mono-parametric vegetation recovery model. The influence of fire damage, pre-fire vegetation density, land-cover type and terrain characteristics in post-fire vegetation recovery time was also assessed.

Large burnt scars are associated with extremely low values of monthly NDVI that persist throughout the vegetative cycle of the year following the fire event. The assessment of burnt areas was based on a K-means spatial cluster analysis, which was applied to NDVI anomaly fields of the hydrological years following each studied fire season, i. e. 2004, 2005 and 2006. Due to the extreme drought of 2004/2005, contamination from fires occurred in 2003 was observed in the analysis of 2004 and 2005 fire seasons, since some pixels from burnt scars of 2003 kept markedly negative values of NDVI anomaly until 2004 or even 2005. The method has revealed to be suitable to detect large fire scars, since burnt areas detected by the cluster analysis on the years of 2003, 2004 and 2005, after removing contamination from previous fires, clearly matched the larger burnt scars identified by AFN (2004; 2005).

A preliminary evaluation of the mono-parametric model's sensitivity to the definition of the starting point was then performed. In some regions, the minimum of lack of greenness was not observed immediately after the fire since, sometimes, the adverse conditions of autumn and winter increase the mortality of surviving vegetation. The model has shown to be particularly affected by the first months following the fire since a small deviation (one or two months) on the starting point led to considerable variations (several months) on estimated recovery times. Thus, the starting point for recovery was set to be the month corresponding to the minimal value of the lack of greenness over the year stating in the beginning of each fire season.

Since the time-series used in Gouveia et al. (2010) did not cover a period sufficiently long to allow fully monitoring of vegetation recovery, the model had to be validated by applying it to the longer time-series available for this work. A comparison between the model's estimations with the 8-year and 11-year time-series, even for burnt areas from 2004 and 2005, allowed the validation of the model for post-fire vegetation recovery. The model has proven to be considerably robust, providing satisfactory

assessment of vegetation recovery even when the time-series is as short as ranging just to 12 months following the fire. However, a correction had to be performed, since some areas presented positive values for the lack of greenness (i.e. NDVI departures from the so-called Gorgeous Year) , which is not consistent with the definition of the Gorgeous Year. In fact, some areas seemed to present changes in the vegetative cycle, indicating possible changes in ecosystem composition or structure, which cannot be assessed using NDVI. The correction procedure simply consisted in removing from the regression analysis the period following the first positive value of the lack of greenness, provided that more than one positive value was observed in the time-series, as they could introduce unrealistic phenological variability in the analysis. Also, the model's sensitivity to missing data amidst the time-series was evaluated. Again the model has proven to be particularly robust, providing recovery time estimations which presented almost no differences from the estimations relying on the complete time-series. This result is valid except in cases when the regeneration process led to changes in ecosystem structure or was disrupted by an extreme natural event, such as drought, or by human intervention. The effect of drought in the application of the model was, therefore, evaluated. It has been shown that drought in the first years of recovery misleads the model's estimations, pushing the regressed curve to lower values. Removal of values corresponding to drought months led to the estimation of considerably shorter recovery times in burnt scars in which vegetation was severely affected by drought.

Four case-studies were selected, in order to perform a more exhaustive analysis of post-fire vegetation recovery, in particular to assess spatial variability and identify the determinant factors of the regeneration process. The mono-parametric model was applied over the burnt scars and to individual pixels, allowing the estimation of overall recovery time and, also, of its spatial distribution for each area. Additional parameters were estimated, such as the level of fire damage – estimated by the fields in May of the year following each fire event – and pre-fire vegetation density – characterized by the median value of NDVI field over the period preceding the fire occurrence. Fire damage and pre-fire conditions fields were compared to recovery time distribution, in order to assess the influence of these parameters in recovery. Land-cover distribution over the burnt scars was also computed, using Corine Land-Cover (2000) database for Continental Portugal, and compared to recovery time, in order to evaluate the importance of specific vegetation post-fire recovery strategies. Finally, terrain characteristics were determined from the GLOBE project Digital Elevation Model, with the aim of assessing the influence of soil moisture conditions in post-fire recovery.

This procedure allowed the distinction of post-fire recovery behaviour and driving factors between different vegetation types. In particular, fire damage has shown to markedly determine coniferous forests regeneration, whereas for broad-leaved forest no marked influence was observed. In broad-leaved forests some degree of relationship between recovery time and pre-fire vegetation density was observed, though not very pronounced. Distinct vegetation recovery rates were observed for different vegetation types, as the burnt scar dominated by broad leaved forest had completely recovered about two years after the fire event, whereas for burnt scars composed by coniferous forests and transitional woodland-shrub clearly distinct phases on the regeneration process were observed. The existence of different stages on recovery is related to distinct recovery rates of transitional woodland-shrub, that tend to recover faster, and coniferous forests which take longer to recover, as assessed by inspecting the composition of recovery time clusters corresponding to these stages. Moreover, the severe drought of 2004/2005 seems to have partially influenced vegetation recovery of the burnt scar from 2003 fire season, delaying a complete recovery. The results are coherent with post-fire recovery characteristics of the studied Mediterranean vegetation types which have been widely demonstrated by several authors (Naveh, 1975; Pausas, 1997; Pérula et al, 2003; Cerdà and Doerr, 2005; Fernandes and Rigolot, 2007).

The influence of soil moisture content and water availability, which are related to terrain characteristics, particularly slope aspect and altitude, was finally evaluated. The effect of these parameters in vegetation recovery was particularly relevant for coniferous forests, which registered a marked contrast in recovery times between Northern and Southern slope aspects. Recovery revealed to be faster in North faced slopes and lower altitudes, as documented in literature (Tsitsoni, 1997; Pausas and Vallejo, 1999; Pausas et al., 2004; Wittenberg et al., 2006).

The consistency of results respecting to the spatial distribution of recovery time and the relevance of driving factors, such as fire regime, vegetation recovery strategies and environmental factors clearly indicate that the methodology used in the present work is adequate for estimating post-fire vegetation recovery times, as well as to evaluate the influence of physical, phenological, and environmental factors on regeneration. The simplicity and the robustness of the proposed methodology is worth being noted, which relies on a linear-regression model that uses a single parameter, avoiding the definition of control plots, and requiring NDVI time-series of modest length and coarse resolution. It is important, nevertheless, to stress that the methodology used neither accounts for individual tree development, nor for ecosystems' structural changes, which may be assessed by means of field studies or other types of satellite imagery that may complement this analysis whenever required.

6. References

AFN, 2010. 5º Inventário Florestal Nacional. Ministério da Agricultura, Pescas e Florestas (in Portuguese).

Arianoutsou, M., Ne'eman, G., 2000. Post-fire regeneration of natural Pinus halepensis forests in the east Mediterranean Basin. In: G. Ne'eman and L. Trabaud, L. (eds.) *Ecology, biogeography and management of Pinus halepensis and P. brutia forest ecosystems in the Mediterranean Basin.* Backhuys, Leiden, NL, 269-290.

Asrar, G., Fuchs, M., Kanemasu, E. T., Hatfield, J. L., 1984. Estimating absorbed photosynthetic radiation and leaf area index from spectral reflectance in wheat. *Agron. J.*, **76**, 300-306.

Catry, F.X., Rego F., Moreira F., Fernandes P.M., Pausas J.G., 2010. Post-fire tree mortality in mixed forests of central Portugal. *Forest Ecology and Management*, **260**, 1184-1192.

Cerdà, A., 1998. Changes in overland flow and infiltration after a rangeland fire in a Mediterranean scrubland. *Hydrological Processes*, **12**, 1031–1042.

Cerdà, A., Doerr, S. H., 2005. The influence of vegetation recovery on soil hydrology and erodibility following fire: an eleven year investigation. *International Journal of Wildland Fire*., **14**[4].

Chuvieco, E., Aguado, I, Yebra, M, Nieto, H., Salas, J., Martín, M. P., Vilar, L., Martínez, J., Martín, S., Ibarra, P., de la Riva, J., Baeza, J., Rodríguez F., Molina J. R., Herrera, M. A., Zamora, R., 2010. Development of a Framework for fire risk assessment using remote sensing and geographic information system Technologies. *Ecol. Model.*, **221**, 46-58.

De Luís, M, Gonzales-Hidalgo, J. C., Raventós, J., 2003. Effects of fire and torrential rainfall on erosion in a mediterranean gorse community. *Land degrade. Delevop.*, **14**, 203-213.

De Luís, M., Baeza, M. J., Raventos, J., Gonzales-Hidalgo, J. C., 2004. Fuel characteristics and fire behavior in mature Mediterranean gorse shrub land, *Int. J. Wildland Fire*, **13**, 79–87.

De Luís, M., García-Cano, M. F., Cortina, J., Raventós, J., González-Hidalgo, J. C., Sánchez, J. R., 2001. Climatic trends, disturbances and short-term vegetation dynamics in a Mediterranean shrubland. *Forest Ecology and Management*, **147**, 25-37.

DeBano, L. F., Neary, D. G., Folliott, P. F., 1998. Fire's Effects on Ecosystems. John Wiley and Sons, New York, 333 pp.

DGRF, 2008. Incêndios Florestais – Portugal. Ministério da Agricultura, Pescas e Florestas (in Portuguese).

Díaz-Delgado, R., Lloret, F., Pons, X., 2003. Influence of fire severity on plant regeneration through remote sensing imagery. *Int. J. Remote Sens.*, **24**(8), 1751–1763.

Díaz-Delgado, R., Pons, X., 2001. Spatial patterns of forest fires in Catalonia (NE of Spain) along the period 1975–1995. Analysis of vegetation recovery after fire. *Forest Ecology and Management*, **147**, 67−74.

Díaz-Delgado, R., Salvador, R., Pons, X., 1998. Monitoring of plant community regeneration after fire by remote sensing. L. Traboud Editor, *Fire management and landscape ecology*. Int. Association of Wildland Fire, Fairfield, WA , 315–324.

Epting, J., Verbyla, D., 2005. Landscape-level interactions of prefire vegetation, burn severity, and postfire vegetation over a 16-year period in interior Alaska. *Can. J. For. Res*. **35**, 1367-1377.

Fernandes, P. M., Rigolot, E., 2007. The fire ecology and management of maritime pine (Pinus Pinaster Ait.). *Forest Ecology and Management*, **241**, 1-13.

Ferran A., Delitti W., Vallejo V.R., 1998. Effects of different fire recurrences in *Quercus coccifera* communities of the Valencia region. Proceedings of the III International Conference on Forest Fire Research, Vol. 2, pp. 1555-1569. Coimbra, 16-20 November 1998.

Fox, D.M., Maselli, F., Carrega, P., 2008.Using SPOT images and field sampling to map burn severity and vegetation factors affecting post forest fire erosion risk. *Catena, Elsevier*, **75**, 326-335.

Garcia-Herrera, R., Paredes, D., Trigo, R. M., Trigo, I. F., Hernández, E., Barriopedro, D., Mendes, M. A., 2007. The Outstanding 2004/05 Drought in the Iberian Peninsula: Associated Atmospheric Circulation. *Journal of Hydrometeorology*, **8**, 483-498.

Goetz, S. J., Fiske, G. J., Bunn, S. G., 2006. Using satellite time-series data set to analyze fire disturbance and forest recovery across Canada. *Remote Sens. Environ.*, **101**, 352–365.

Gouveia, C., Trigo, R.M., DaCamara, C.C., 2009. Drought and vegetation stress monitoring in Portugal using satellite data. *Natural Hazards and Earth System Sciences*, **9**, 185–195.

Gouveia C., DaCamara C.C, Trigo R.M., 2010. Post fire vegetation recovery in Portugal based on SPOT-VEGETATION data. *Natural Hazards and Earth System Sciences*, **10**, 673-684.

Hagolle, O., Lobo, A., Maisongrande, P., Duchemin, B. & De Pereira, A., 2005. Quality assessment and improvement of SPOT/VEGETATION level temporally composited products of remotely sensed imagery by combination of VEGETATION 1 and 2 images. *Rem. Sens. Environ.*, **94** (2), 172–186.

Hartigan, J. A., Wong, M. A., 1979. Algorithm AS 136: A K-Means Clustering Algorithm. *J. Roy. Stat. Soc. C-App.*, **28**(1), 100–108.

Hastings, D. A., Dunbar, P. K., Elphingstone, G. M., Bootz, M., Murakami, H., Maruyama, H., Masaharu, H., Holland, P., Payne, J., Bryant, N. A., Logan, T. L., Muller, J.-P., Schreier, G., MacDonald, J. S. (eds.), 1999. The Global Land One-kilometer Base Elevation (GLOBE) Digital Elevation Model, Version 1.0. National Oceanic and Atmospheric Administration, National Geophysical Data Center.

Holben, B. N., 1986. Characteristics of maximum-value composite images from temporal AVHRR data. *Int. J. Rem. Sens*., **7**, 1417–1434.

Hope, A., Tague, C., Clark, R., 2007. Characterizing post-fire vegetation recovery of California chaparral using TM/ETM+ time-series data. *Int. J. Remote Sens.*, **28**(6), 1339–1354.

Houghton JT, Meiro Filho LG, Callander BA, Kattenburg A, Maskell K (eds), 1996. Climate Change 1995. *The Second Assessment Report of the IPCC*. Cambridge University Press, Cambridge.

Huete, A. R., 1988. A soil adjusted vegetation index. *Remote Sens. Environ.*, **25**, 295–309.

Inbar, M., Wittenberg, L., Tamir, M., 1998. Soil erosion and forestry management after wildfire in a Mediterranean woodland, Mt. Carmel, Israel. *Int. J. of Wild. Fire*, **7**, 285–294.

JRC-EC, 2009. Forest Fires in Europe 2009, Report No. 10. Institute for Environment and Sustainability, European Comission.

Julien Y., Sobrino J. A., Verhoef, W., 2006. Changes in land surface temperatures and NDVI values over Europe between 1982 and 1999. *Remote Sens. Environ.*, **103**(1), 43–55.

Karnieli, A., Bayasgalan, M., Bayarjargal, Y., Agam, N., Khudulmur, S., Tucker, C. J., 2006. Comments on the use of the Vegetation Health Index over Mongolia. *Int. J. Remote Sens.*, **27**(10), 2017–2024.

Kaufman, Y. J., Tanré, D., 1992. Atmospherically resistant vegetation index (ARVI) for EOS-MODIS. *IEEE Trans. Geosc. Rem. Sens.*, **30** , 261-270.

Lloret, F., 1998. Fire, canopy cover and seedling dynamics in Mediterranean shrubland of northeastern Spain. *J. Veg. Sci.*, **9**, 417-430.

Loepfe, L., Martinez-Vilalta, J., Oliveres, J., Piñol, J., Lloret, F., 2010. Feedbacks between fuel reduction and landscape homogenisation determine fire regimes in three Mediterranean areas. *Forest Ecology and Management*, **259**, 2366-2374.

Los, S. O., 1998. Linkages between global vegetation and climate: an analysis based on NOAA-Advanced Very High Resolution Radiometer Data. Ph.D. thesis, Vrije Universiteit, Amsterdam, 179 pp.

MacQueen, J. B., 1967. Some methods for classification and analysis of multivariate observations. *Proc. 5th Berkeley Symposium on Mathematical Statistics and Probability 1*, University of California Press, 281–297.

Maisongrande, P., Duchemin, B. & Dedieu, G., 2004. VEGETATION/SPOT – An Operational Mission for the Earth Monitoring: Presentation of New Standard Products. *Int. J. Remote Sens*., **25**, 9–14.

Minchella, A., Del Frate, F., Capogna, F., Anselmi, S., Manes, F., 2009. Use of multitemporal SAR data for monitoring vegetation recovery of Mediterranean burned areas. *Rem. Sens. Environ.*, **113**, 588–597.

Moreira, F., Catry, F., Lopes, T., Bugalho, M. N., Rego, F., 2009. Comparing survival and size of resprouts and planted trees for post-fire forest restoration in central Portugal. *Ecological Engineering*, **35,** 870–873.

Moreno, J.M., Oechel, W.C. (eds.), 1995. *The Role of Fire in Mediterranean-Type Ecosystems.* Springer–Verlag, New York, USA.

Myneni, R. B., Hall, F. G., Sellers, P. J., Marshak, A. L., 1995. The interpretation of spectral vegetation indexes. *IEEE Trans. Geosc. Rem. Sens.*, **33** (2).

Naveh. Z., 1975. The evolutionary significance of fire in the Mediterranean region. *Plant Ecology*, **29**, 3, 199-208.

Naveh, Z., 1995. The role of fire and its management in the conservation of Mediterranean ecosystems and landscapes. Moreno, J.M., Oechel, W.C.(eds.), *The Role of Fire in Mediterranean-Type Ecosystems.* Springer–Verlag, New York, USA, pp 163–185.

Nunes, M. C. S., Vasconcelos, M. J., Pereira, J. M. C., Dasgupta, N., Alldredge, R. J., Rego, F. C., 2005. Land Cover type and fire in Portugal: Do fires burn land cover selectively?, *Landscape Ecol.*, **20**, 661–673.

Pausas, J.G., 1997. Resprouting of cork-oak (*Quercus suber* L.) after fire in NE Spain. *J. Veg. Sci*., **8**, 703-706.

Pausas, G. J., Vallejo, V. R., 1999. The role of fire in European Mediterranean Ecosystems. In: E. Chuvieco, (eds.), *Remote sensing of large wildfires in the European Mediterranean basin*, Springer-Verlag, 3–16.

Pausas, J.G.,Ribeiro, E., VAllejo, R., 2004. Post-fire regeneration variability of Pinus halepensis in the eastern Iberian Peninsula. *Forest ecology and management,* **203**,251-259.

Pereira, M. G., Trigo, R. M., DaCamara, C. C., Pereira, J. M. C., Leite, S. M., 2005. Synoptic patterns associated with large summer forest fires in Portugal, *Agr. Forest Meteorol*., **129**(1–2), 11–25.

Pérula, V. G., Cerrillo, R. M. N., Rebollo, P. F., Murillo, G. V., 2003. Postfire regeneration of Pinus Pinea L. and Pinus Pinaster Aiton in Andalucia (Spain). *Environmental Management*, **31**(1), 86-99.

Pyne, S. J., Andrews, P. L., Laven, R. D., 1996. Introduction to Wildland Fire, 2nd edn. John Wiley and Sons: New York.

Rahman, H., Dedieu, G., 1994. SMAC: a simplified method for the atmospheric correction of satellite measurements in the solar spectrum, *Int. J. Remote Sens.*, **15**, 123–143.

Retana, J., Espelta, J. M., Habrouk, A., Ordoñez, J. L., de Sola- Morales, F., 2002. Regeneration patterns of three Mediterranean pines and forest changes after a large wildfire in northeastern Spain. *Ecoscience* **9**, 89-97.

Riaño, D., Chuvieco, E., Ustin, S., Zomer, R., Dennison, P., Roberts, D. A., 2002. Assessment of vegetation regeneration after fire through multitemporal analysis of AVIRIS images in the Santa Monica Mountains, *Remote Sens. Environ.*, **79**, 60–71.

Röder, A., Hill, J., Duguy, B., Alloza, J. A., Vallejo, R., 2008. Using long time series of Landsat data to monitor fire events and postfire dynamics and identify driving factors. A case study in the Ayora region (eastern Spain), *Remote Sens. Environ.*, **112**, 259–273.

Rouse, J.W., Haas, R.H., Schell, J.A., Deering, D.W., Harlan, J.C., 1974. Monitoring the vernal advancement and retrogradation (greenwave effect) of natural vegetation. *NASA/GSFC Type III Final Report*, Greenbelt, Md. 371 pp.

Sawyer, C. N., McCarty, P. L., Parkin, G. F., 2002. *Chemistry for Environmental Engineering and Science*, 5th ed., New York, McGraw-Hill, 752 pp.

Sellers P.J., Berry J.A., Collatz G.J., Field C.B., Hall F.G., 1992. Canopy reflectance, photosynthesis and transpiration, III. A reanalysis using enzyme kinetics—electron transport models of leaf physiology. *Remote Sens. Environ.*, **42**, pp. 187–216.

Sellers, P. J., Dickinson, R. E., Randall, D. A., Betts, A. K., Hall, F. G., Berry, J. A., Collatz, G. J., Denning, A. S., Mooney, H. A., Nobre, C. A., Sato, N., Field, C. B. & Henderson-Sellers, A., 1997. Modeling the exchanges of energy, water, and carbon between continents and the atmosphere. *Science*, **275**, 502–509.

Shakesby, R. A., Coelho, C. O. A., Ferreira, A. D., Terry, J. P., Walsh, R. P. D., 1993. Wildfire impacts on soil erosion and hydrology in wet Mediterranean forest, Portugal. *Int. J. of Wildland Fire* **3**, 95–110.

Stockli, R., Vidale, P. L., 2004. European plant phenology and climate as seen in a 20-year AVHRR land-surface parameter dataset. *Int. J. Remote Sens*., **25**, 3303–3330.

Thornes, J., 1990. The interaction of erosion and vegetation dynamics in land degradation: spatial outcomes.*Vegetation and Erosion*, Wiley, New York, 41–54.

Trigo R.M., Pereira, J.M.C., Pereira, M.G., Mota B., Calado, M.T., DaCamara C.C., Santo, F.E., 2006. Atmospheric conditions associated with the exceptional fire season of 2003 in Portugal. *International Journal of Climatology*, **26**(13), 1741–1757.

Tsitsoni, T., 1997. Conditions determining natural regeneration after wildfires in the *Pinus halepensis* forests of Kassandra Peninsula (North Greece). *Forest Ecology and Management*, **92,** 199-208.

Tucker, C. J., 1979. Red and photographic infrared linear combinations for monitoring vegetation. *Remote Sens. Environ.*, **8**(2), 127–150.

Turner, M., O'neill, R. V., Gardner, R. H., Milne, B. T., 1989. Effects of changing spatial scale on the analysis of landscape pattern. *Landscape Ecology*, **3** (3/4), 153-162.

Vasconcelos, M.J.P., Silva, S., Tomé, M., Alvim, M., Pereira, J.M.C., 2001. Spatial Prediction of fire ignition probabilities: comparing logistic regression and neural networks. *Photogrammetr. Eng. Remote Sensing* **67**, 73–81.

Vázquez, A., Moreno, J. M., 2001. Spatial distribution of forest fires in Sierra de Gredos (Central Spain). *Forest Ecology and Management*, **147**, 55-65.

Vicente-Serrano, S. M., Heredia-Laclaustra, A., 2004. NAO influence on NDVI trends in the Iberian peninsula (1982–2000). *Int. J. Remote Sens.*, **25**(14), 2871–2879.

Wittenberg, L., Malkinson, D., Beer, O., Halutzy, A., Tesler, N., 2007. Spatial and temporal patterns of vegetation recovery following sequences of forest fires in a Mediterranean landscape, Mt. Carmel Israel, *Catena, Elsevier*, **71**(1), 76–83.